# Improving global glacier modelling by the inclusion of parameterised subgrid hypsometry within a three-dimensional, dynamical ice sheet model.

O.J.H. Browne

Supervised by Dr J. Gregory

September, 2004

## abstract

This study is motivated by the need to make predictions for how global glacier mass responds to climate change on timescales comparable to those of the dynamic adjustment of glaciers. Application of a model that parameterises subgrid mass balance as a function of subgrid topography is used. It is shown that this leads to the model being able to predict realistic stable states for glaciers. Sensitivity tests are applied as well as a $4 \, \mathrm{x} \, CO_2$ warming which leads to a sea level rise equivalent to $0.07 \, m$ of glacier melt.

## Declaration

I confirm that this is my own work and the use of all material from other sources has been properly and fully acknowledged.

## Acknowledgements

# Contents

# Chapter 1

# Introduction

## 1.1 An overview of this study

The study begins by considering how glaciers work conceptually, why improvements in modelling them are of interest, and how such improvements will be attempted within this study. Chapter 2 examines the processes that are involved in glaciers in more depth, previous attempts to model them and their weaknesses, and closes by describing the equations involved in modelling the dynamics and thermodynamics of glaciers. Discussion in chapter 3 focuses on the two main parameterisations used: the degree-day scheme and the subgrid hypsometric scheme. It is the inclusion of this latter parameterisation that led to the choice of model because of the improvements to glacier modelling it can offer. Chapter 4 covers the approaches used to numerically approximate the equations in chapter 2. The choices of input data and experiments are discussed in Chapter 5. The results of these tests, on the effectiveness of the subgrid hypsometric parameterisation, and the consequences on response of glaciers to climate change are presented in chapter 6. Conclusions are drawn, and further work is considered in chapter 7.

## 1.2 Notation

The notation in the document follows that of mathematical conventions: the over-bar $\bar{x}$ denotes the mean of $x$, subscripts $_{i,j,k}$ and superscript $^{m}$ denote spatial and time co-ordinates. Superscripts $^{I}$ and $^{B}$ denote whether the term (usually elevation) refers to ice surface or base topography respectively. For operations and vectors $_{j}$ means the two-dimensional case whereas

$k$ is used for the three-dimensional case. Time is denoted by $t$, temperature by $T$ and $(u, v, w)$ are the components of the three-dimensional velocity field, $v_k(\lambda, \theta, z, t)$, in which $\lambda$ is the longitude, $\theta$ is the co-latitude and $z$ is the elevation. The two-dimensional equivalent is $v_k(\lambda, \theta)$ with components $(u, v)$.

Measures of height or length in this document are metric and wherever $a$ appears as a unit it refers to annum. The earth is split into $360\,°$ of longitude, and $180\,°$ of latitude. The terms "minutes" and "arcsecs" are measures of distance, in spherical co-ordinates. Each degree is then split into 60 minutes, and each minute is split into 60 arc-seconds. The co-latitude is the angle between any latitude and the North Pole. London has a latitude of $51\,°$N, which is a co-latitude of $39\,°$, and Sydney has a latitude of $34\,°$S, which is a co-latitude of $124\,°$.

## 1.3   What is a Glacier?

The OED defines a glacier as "A slowly moving mass of ice formed by accumulation and compaction of snow on mountains or near the poles". The health of an individual glacier can be measured by its mass balance; this is the difference between how much ice is gained during the year (accumulation), and how much is lost (ablation). When considering a mountain glacier in balance, as in Figure 1.1, then at high elevations there exists an area of net accumulation, and at low elevations there is an area of net ablation. This is because as altitude increases, the air temperature falls, and hence precipitation is more likely to fall as snow and less likely to melt at the surface, and vice versa as altitude decreases.

To compensate for these net imbalances there is a flux of ice down slope, so that the snow that falls on the top of a glacier today, will compact to form ice (in various stages), then be passed down slope, and eventually melt. The speed of the ice varies, generally moving as "sheet flow $(0 - 80\,m\,a^{-1})$[1], but in regions known as streams moving much more rapidly - Ice Stream B in West Antarctica moves at up to $800\,m\,a^{-1}$. Stream flow will be considered in more detail later. Sheet flow is not constant across a glacier, but instead is partly dependent on the surface mass balance. This is the amount of accumulation and ablation averaged over the surface area of a glacier or ice mass.

Antarctica for instance is cold enough to undergo no melting at all. There is also relatively

---

[1]Dahl-Jensen, 1989
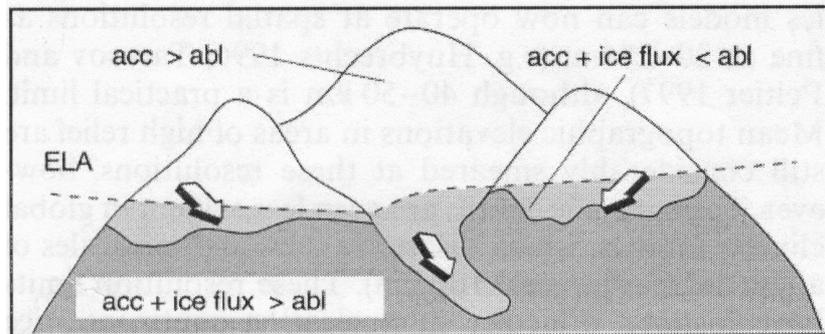
Figure 1.1: from Marshall & Clarke, 1999

little snowfall, with most occurring at the margins[2], which is then averaged over a large surface area. A glacier in the Alps on the other hand has a large amount of melting and snowfall in comparison to its surface area. To keep in balance the Alpine glaciers have to move their ice more quickly from peak to terminus. Thus the timescale for this process varies, from $10 - 100$ years for small glaciers, through to hundreds of thousands of years for the large ice sheets.

There are several major ice-mass forms, the largest of which is an ice sheet with thicknesses of up to several thousand metres. It dominates its underlying topography and its outer surface is dictated by its internal dynamics. Bed topography is usually depressed under an ice sheet, as the magma in the mantle of the earth will be displaced by the great weight of ice atop it. The vertical adjustment of the crust is known as isostasy.

In terms of land ice, ice caps are the next largest although the distinction between ice caps and glaciers is vague; ice caps are generally considered as having areas greater than $\sim 1000 km^2$ and a glacier is any land based ice smaller than this. The distinction between a glacier and an ice sheet is that the surface of a glacier is strongly influenced by its underlying topography. This difference is essentially a difference in scale; glaciers are on the $1 \sim 100 km$ scale, whereas ice sheets are on the $\sim 1000 km$ scale, and as such the two ice-mass types have historically been modelled separately.

In the oceans there are two forms of ice-mass; the first is sea-ice, which forms when the sea surface temperature falls low enough $(\sim -1.8\,°C)$; large amounts of sea ice are found in the Arctic Ocean. In changing states from water to ice most of the salt content is removed, and this combines with the decrease in density as it changes states to make the ice lighter than the

---

[2]cold air can support less water, which is one of the reasons that central Antarctica is dry
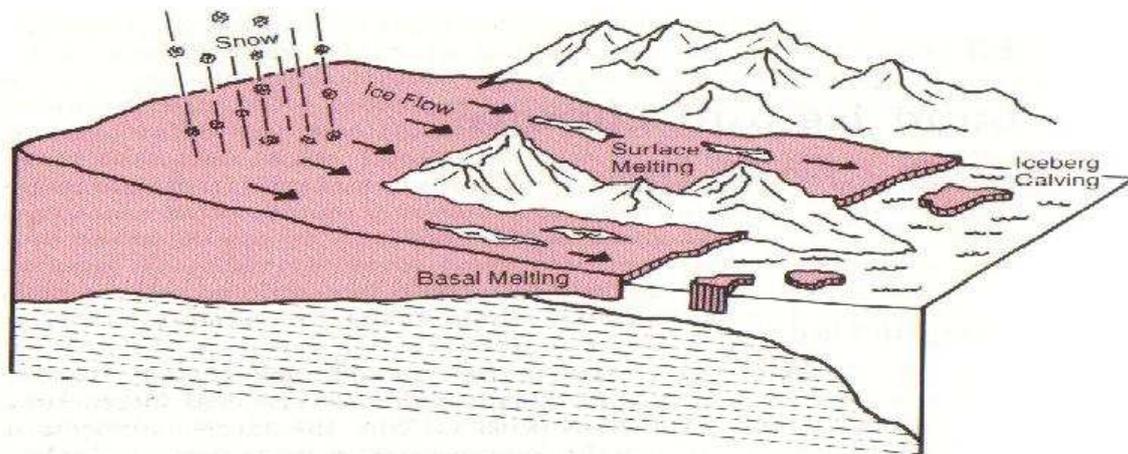
Figure 1.2: from Trenberth, 1999

surrounding sea water, which is why sea-ice floats.

The second form of ice-mass that occurs over the sea is an Ice Shelf, as illustrated in Figure 1.2. It is like an ice sheet that has floated out to sea; it is distinct from sea ice because some part of it remains attached to land - grounded - even though this may be below sea level, such as the Larsen B ice shelf in Antarctica. At the terminus of an ice shelf, as illustrated in Figure 1.2 the ice may disintegrate into floating icebergs. The production of icebergs, known as calving can occur wherever a glacier or ice sheet meets the sea, or where an ice shelf exists. Calving is key in modelling Antarctica because under present climatic conditions it is the only form of mass loss that occurs on this ice sheet.

Ice shelves and sea-ice must both displace sea water to float and so the sea level has already adjusted to carrying their mass. If they should melt sea levels would remain the same, and so we do not need to take direct account of them when modelling sea level rise. The loss of sea ice can feedback on to sea levels by the albedo effect, which is discussed in section 2.1, but this effect is beyond the scope of this study.

## 1.4   Why are we interested in Glaciers?

Sea levels affect millions of people; a large portion of the population lives on or near the coast. Therefore improvements in any of the estimates of contributions to sea level rise are of interest. With the increased temperatures and change in water and land use associated with climate
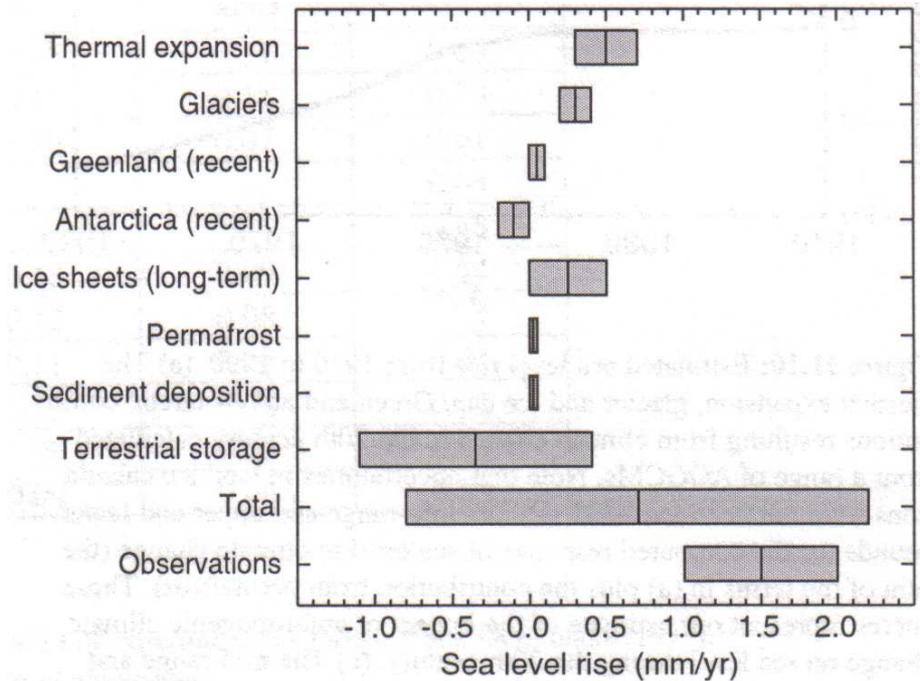
Ranges of uncertainty for the average rate of sea level rise from 1910 to 1990 and the estimated contributions from different processes.

Figure 1.3: from the IPCC's third assessment report, chapter 11

change the sea level is changing and will continue to so. Figure 1.3 details contributions to sea level rise over the next 500 years. The biggest contributor by far is thermal expansion, which is the expansion of water in response to heating. The terrestrial contribution is affected by many factors, including: the storing of water on land in reservoirs behind hydroelectric dams and lakes; the increased amounts of runoff in urbanised areas and in deforested regions; and the change in land ice mass. The ice contribution can be broken into (i) glaciers and ice caps, (ii) Greenland and (iii) Antarctica. Their volumes and the amount that sea levels would rise if they were to completely melt are listed in Figure 1.4. However, total melt is unlikely, and mis-guiding as a measure because it would indicate that Antarctica is the biggest concern to sea level rise. However, a small increase in temperature and precipitation would not lead to melting because Antarctica is too cold for this. Thus the increased precipitation expected with climate change will accumulate, lowering sea levels, until Antarctica reacts dynamically; increasing the flux of ice to its margins and thus its rate of calving.

The length of dynamic adjustment can be thought of as the 'turn-over' time of an ice-mass.

In Antarctica's case the flux of ice is low compared to its total volume, so it takes a long time for changes to filter through. Raper et al. (2000) show that the turnover timescale can be expressed by,

$$\text{Dynamic Adjustment Timescale} \propto \frac{\text{total volume}}{\text{accumulation rate}} \quad . \tag{1.1}$$

However, when the climate changes, the mass balance changes immediately, so the dynamic adjustment timescale explains why ice-masses lag, to varying extents, behind climate change. This is important to modelling of sea level because people are interested in what happens over the next hundred years rather than the equilibrium change which would take Greenland thousands of years and Antarctica even longer. For instance the accumulation over Greenland is roughly equivalent to that over all the glaciers and ice caps in the world. However, Figure 1.4 shows Greenland's volume to be far greater, and thus the dynamic adjustment timescale for glaciers and ice caps is much smaller than that of Greenland. This means the glaciers and ice caps will reach find a new balance level quicker than the ice sheets.

If climate perturbations over the glaciers and ice caps of the world were comparable to those over ice sheets, then the changes in accumulation over each would also be comparable. Since accumulation over glaciers is roughly equal to that over Greenland, and accumulation is one half of the mass balance, the deficits in mass balance would be comparable across the two. This means that in the short term, before dynamical changes occur, the two forms of ice-mass would give similar contributions to sea level rise, despite the much greater size of the ice sheets. In addition to this both ice-sheets are in very cold climates. This means that the amount their mass balance will react to changes in temperature is very low[3]. In the case of Antarctica this is as good as zero and for Greenland also small. This means the ice sheets actually contribute less than the glaciers and, in fact, Antarctica contributes negatively.

The nature of climate change will accentuate these changes. Warming is projected to be non-uniform, with the greatest increases in temperature taking place in the high-latitudes, especially in the northern hemisphere, where most glaciers reside. This is thought to be because the reduction in snow and sea ice cover at high-latitudes causes an ice-albedo feedback (section 2.1) and because the southern hemisphere has a much larger proportion of ocean which will absorb some of the warming. The precipitation field is similarly variable, with most projections showing the largest increases occurring in the tropics, a decrease in the sub-tropics and then

---

[3]explained in more detail in section 2.1.1

| | Glaciers | Ice caps | Glaciers and ice caps [a] | Greenland ice sheet [b] | Antarctic ice sheet [b] |
|---|---|---|---|---|---|
| Number | >160 000 | 70 | | | |
| Area ($10^6$ km$^2$) | 0.43 | 0.24 | 0.68 | 1.71 | 12.37 |
| Volume ($10^6$ km$^3$) | 0.08 | 0.10 | $0.18 \pm 0.04$ | 2.85 | 25.71 |
| Sea-level rise equivalent [d] | 0.24 | 0.27 | $0.50 \pm 0.10$ | 7.2[c] | 61.1[c] |
| Accumulation (sea-level equivalent, mm/yr) [d] | | | $1.9 \pm 0.3$ | $1.4 \pm 0.1$ | $5.1 \pm 0.2$ |

Data sources: Meier and Bahr (1996), Warrick *et al.* (1996), Reeh *et al.* (1999), Huybrechts *et al.* (2000), Tables 11.5 and 11.6.

[a] Including glaciers and ice caps on the margins of Greenland and the Antarctic Peninsula, which have a total area of $0.14 \times 10^6$ km$^2$ (Weideck and Morris, 1996). The total area of glaciers and ice-caps outside Greenland and Antarctica is $0.54 \times 10^6$ km$^2$ (Dyurgerov and Meier, 1997a). The glaciers and ice caps of Greenland and Antarctica are included again in the next two columns.

[b] Grounded ice only, including glaciers and small ice caps.

[c] For the ice sheets, sea level rise equivalent is calculated with allowance for isostatic rebound and sea water replacing grounded ice, and this therefore is less than the sea level equivalent of the ice volume.

[d] Assuming an oceanic area of $3.62 \times 10^8$ km$^2$.

Figure 1.4: from the IPCC's third assessment report, chapter 11

a small increase at mid and high latitudes (Noda and Tokioka (1989), Murphy and Mitchell (1995), and Royer et al. (1998)). The decrease in the sub-tropics is attributed to increased tropospheric stability in the warmer climate.

The increased precipitation levels, expected to average 2% per degree of any temperature increase (Van der Wal and Wil), will not be sufficient to maintain balance. Mass balance modelling suggests that for a glacier to stay in balance it would need a 20% to 35%[4] increase in precipitation per 1 °K rise. On the global scale, temperature increases are likely to dominate the balance by far, which means that the total glacial melt rate will continue to rise.

Current projections for the contributions of glaciers and ice-caps to sea level rise, shown in Figure 1.3 suggest a figure of 0.16m over the next century, but with an error margin of 40%. This margin, coupled with the importance of sea level rise estimates to populations worldwide, motivates an investigation of possible improvements to this estimate.

Van der Wal and Wil (2001) show that using mass balance models without taking account of changes in surface area leads to an overestimate of sea level rise by 19%. Whilst their method is an improvement on others, it is still limited in two key ways. Firstly it has no dynamics, which as shall be shown in chapter 2, are important for improving glacial melt estimates and essential for modelling stabiisation of glaciers. Secondly the application of mass balance models to global glacier volumes is limited by a lack of meteorological and mass balance data. Estimates must be made by assuming certain regions share the similar mass balance properties. This makes projecting global glacier contributions to sea level rise inaccurate.

---

[4]Oerlemans, 1981 and Raper et al, 2000 respectively.

Dynamical models offer a solution to this situation, but have been previously excluded because the scale at which they run is too large, and when brought down to a scale suitable for glaciers they then have the same problems with lacking sufficient meteorological data. However, the development by Marshall and Clarke (1999) of a subgrid parameterisation that captures the detail of the terrain and its consequential meteorological effects allows dynamical models to be used for global glacier volume estimates for the first time.

# Chapter 2

# Ice-mass Modelling Theory

## 2.1 Accumulation versus Ablation

Precipitation onto an ice-mass may either land as snow/hail, or rain. The part that falls as snow/hail, and the part of the rain that froze upon impact may survive a whole year to become firn. It may remain in place and go through several further stages of compaction under subsequent layers of precipitation[1], until it reaches the necessary pressure ($830 kg\, m^{-2}$) for its internal crystals to align to become ice. Alternatively it may melt on the surface. This melt water, along with the rain that did not freeze, may then evaporate or run-off; or it may soak into the snowfall and refreeze. The accumulation in a given year comprises the part of the precipitation that did not evaporate or run-off.

Ablation may occur in three ways: surficial melting, calving and basal melting. The first is the part of the surface melt-water that does not refreeze. Calving was defined on page 7. Basal melting is caused by extreme pressure at the base and the geothermal flux released by the Earth. Water, unlike most materials, expands when moving to a solid. The consequence of this is that external pressure depresses the melting temperatures. The value to which they are depressed, known as the pressure melting point, can be approximated as a function of depth,

$$T_{pmp} = T_0 - \beta(H - z), \tag{2.1}$$

where $H$ is the thickness of the ice mass, $z$ is the distance below the surface, $T_0$ is the melting

---

[1]see Patterson, 1994, Chapter 2

point of ice and $\beta$ is derived from the clasius-claperyon equation. Basal flow is important in ice sheets as it is the dominant factor in stream flow (see section 2.3.2) but in glaciers basal flow is much less common. This is because glaciers generally do not develop the necessary thickness to reach the pressures and thermal insulation required to melt ice at their base.

Mass balance is the difference between the accumulation and the ablation over a glacier; when the mass balance is zero, the mass of the glacier is not changing. The specific mass balance - the form most ice-sheet models use - is the mass balance divided by the area of the glacier. Specific mass balance varies across the length of a glacier, with negative values at low levels where ablation dominates, zero at the equilibrium level altitude (ELA) and positive values at the high levels where accumulation dominates. The specific mass balance profile also varies with latitude and climate. The ELA can be thought of as a marker for the mass balance profile. In the subtropics it is at high elevations ($> 4000\,\text{m}$) and gradually falls to low elevations ($< 1000\,m$) at the poles. Stable glaciers which receive a lot of precipitation, and so have a high turnover, will have steep mass balance profiles, whereas glaciers in the drier polar and sub-polar regions have much more gentle profiles.

Knowledge of the health of a glacier requires knowledge of climatic conditions and knowledge of how these conditions translate into the mass balance. One method of calculating mass balance is energy balance modelling, the approach adopted by Oerlemans and Fortuin (1992). In their model the balance, $B$, is given by

$$B = \int_{year} \underbrace{(1-f)min(0, -\Psi L)}_{\text{ablation}} + \underbrace{p^*}_{\text{accumulation}} dt. \tag{2.2}$$

Accumulation of solid precipitation is given by $P^*$. Ablation is obtained by finding the fraction of surface melt-water that does not refreeze, $(1-f)$, where $f$ is the fraction that does refreeze. The term $min(0, -\Psi L)$ multiplies the energy balance at the ice-snow interval, $\Psi$, by the latent heat required to melt ice, $L$; when this is positive, melting occurs. The computation of energy balance requires knowledge of solar radiation (shortwave), atmospheric radiation (longwave), turbulent fluxes of heat and moisture and energy used for heating the snow or ice layers.

Computation of the radiation components requires knowledge of surface albedo amongst other factors. The albedo of an object is a measure of how reflective it is: white, shiny objects will have a higher albedo (near 1) than dark, dull objects (near 0). Ice is very reflective compared

to most other surfaces on Earth. This is important because in forest terrain, sunlight, which is shortwave radiation, will be absorbed by the ground and heat, which is longwave radiation, will be emitted; this warms the atmosphere. Over an ice mass, however, most shortwave radiation is reflected, due to its high albedo, and so there is less heating of the atmosphere. This is a positive feedback process which means it encourages whatever the ice mass is doing. In periods of growth the atmosphere is cooled which promotes further growth, whereas in periods of retreat the reduction in the albedo-effect warms the atmosphere, encouraging further retreat. Ice albedo decreases down a glacier and through the course of the summer melt season.

The problem with using energy balance models on a global scale is that the detailed information of surface fluxes is only available for a few glaciers worldwide. Furthermore, the climate models that are used to generate projections of future climate scenarios do not produce this level of detail. For this reason, temperature index methods are used. These parameterise ablation and the fraction of precipitation to fall as snow as functions of temperature[2]. This reduces the problem of knowledge of climatic conditions to knowledge of temperature and precipitation, which can currently be modelled on a global scale at a resolution of $10 - 100\,km$.

### 2.1.1 Mass Balance Sensitivity

An ice sheet starts life as a glacier; effectively they are the same thing, with the same rules, just applied on a different scale. It has been established that energy balance modelling generally requires more information than is currently available, and that temperature index methods allow us to limit our dependence to temperature and precipitation modelling. On a global scale the approach of nesting regional climate models in general circulation models (Hostetler and Clark, 1997) and downscaling of GCM output (Glover, 1998) has improved the realism on the $10 - 100km$ scale. However, glacier models at present require a level of detail that could not function with this little detail. Moreover, of the +160,000 glaciers in the world, only 100 have been mass balance records greater than 5 years, and only 40 have records longer than 20 years.

One way around this is to group glaciers by their mass balance sensitivity - that is how much their mass balance changes per degree change in temperature, and so maximise the knowledge we have. Mass balance sensitivity varies across the globe; summer temperature increases are generally the most important increases for glaciers because the winter temperatures are suffi-

---

[2]more details on temperature index methods are given in section 3.2
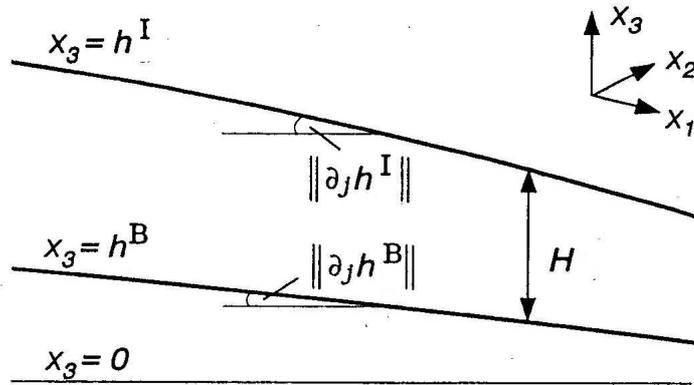
Figure 2.1: from The UBC Ice Sheet manual

ciently low that increases do not cause melting.  However, for low-latitude glaciers the annual average rise is more crucial.  The problem this runs into is that whilst we have a good idea of the area and volumes of glaciers in these separate regions, we lack accurate measures of the specific mass balances.

## 2.2   Ice Thickness, the first prognostic variable

The spatial and temporal evolution in thickness of an ice mass gives an easy to grasp measure of what the ice mass is doing and as such is one of two key prognostic outputs used in most contemporary models, the other being ice velocity.

The diagram above shows a simple ice sheet profile, with $h_a^I$ representing the ice sheet surface, $h^B$ representing the bed, and 0 taken as a large scale base marker, say a geoid of the earth, or sea level.  The thickness of the ice sheet is given by $H = h^I - h^B$, and the mass balance equation gives the evolution of the sheet ice; Ice thickness;

$$\frac{\partial H}{\partial t} = \dot{b} - \bigtriangledown.(\bar{v}_j H) \tag{2.3}$$

In equation (2.3) $t$ is time, $v$ denotes the velocity, and $\dot{b}$ is the mass balance term.

## 2.3 Ice Dynamics

Ice can flow by internal deformation or by basal interactions. The rate of flow is variable, but can be segmented into two main forms, stream flow and sheet flow, with stream flow an order of magnitude or more greater that sheet flow.

### 2.3.1 Sheet Flow

If we consider an example where our ice-mass is frozen to its bed, as is the case for glaciers most of the time, then the velocity is zero at the bed, and sheet flow is the internal deformation of the ice; the plastic response of the ice to the pull of gravity. The deformation, known as viscous creep deformation, occurs as ice crystals slide over one another and change shape (see Patterson, chapter 5), with movement increasing with height above the bed. For large ice sheets there may be local, small scale basal flows occurring, which are on a similar order of magnitude to the viscous creep fluxes (Marshall 1997c). On the synoptic grid cell scale however, the basal movement is sufficiently small and uncoordinated to mean the ice sheet is mostly coupled to its bed and sheet ice flow is dominated by creep deformation.

Ice sheet flow is approximated to flow purely by vertical shear deformation. This approach, in which the longitudinal and horizontal shear deformations are ignored, is used in most ice sheet models (Huybrechts, 1986, Deblonde, 1990, Payne, 1995). The numerics were first devised by Mahaffy (1974, 1976), the assumptions involved are detailed by Hutter (1983) and a fuller explanation of the stresses involved is given in Patterson (chapter 5). The resulting equations are known as the Shallow-Ice equations, and allow ice velocities to be expressed as a function of local ice thickness and surface slope.

Assuming ice to be incompressible, then it is the stress deviators, rather than the stresses themselves that cause deformation (Patterson, 1994, p90). We can define a strain rate tensor;

$$\dot{\epsilon}_{ik} = \frac{1}{2}\left(\frac{\partial v_i}{\partial x_k} + \frac{\partial v_k}{\partial x_i}\right), \tag{2.4}$$

and, for internal ice pressure $p^I$, a deviatoric stress tensor,

$$\dot{\sigma}_{ik} = \sigma_{ik} - \sigma_{kk}\delta_{ik} = \sigma_{ik} + p^I\delta_{ik}. \tag{2.5}$$

Glen (1955,1958) related strain rates to deviatoric stresses in ice. It is an empirical relation, but has a good physical basis,

$$\dot{\delta}_{ik} = A(T^I)(\Sigma_2)^{(n-1)/2}\sigma_{ik}, \tag{2.6}$$

with $T$ as the temperature of the ice. The flow law exponent, $n$, is usually set to 3 in ice sheet studies, but for which field studies still show much disagreement over (Patterson, 1994, p95). The second invariant of the deviatoric stress tensor, $\Sigma_2$, is given by,

$$\Sigma_2 = \frac{1}{2}\,\sigma_{ik}\sigma_{ki}. \tag{2.7}$$

Arrhenius' term, $A(T^I)$, in Glen's flow law is an inverse viscosity term, and is given by the Arrhenius equation,

$$A(T^I) = A_0 exp\,\left(\frac{-Q}{R_{gas}T^I}\right), \tag{2.8}$$

where $Q$ is a creep activation energy - there is a minimum level of energy required before deformation occurs - $R_{g}as$ is the ideal gas law constant, and $A_0$ is a constant found by experimentation.

The vertically-integrated momentum equations, with Glen's flow law applied, then give the horizontal velocity components,

$$u(z) \;\;=\;\; u(h^B) - 2(\rho^I g)^n\,\|\partial_j h^I\|^{n-1}\,\frac{\partial h^I}{\partial x_1}\,\int_{h^B}^{z} A(T^I)(h^I - z)^n dz, \tag{2.9}$$

$$v(z) \;\;=\;\; v(h^B) - 2(\rho^I g)^n\,\|\partial_j h^I\|^{n-1}\,\frac{\partial h^I}{\partial x_2}\,\int_{h^B}^{z} A(T^I)(h^I - z)^n dz. \tag{2.10}$$

Vector $\partial_j h^I$ has $L_2-norm$ $\|\partial_j h^I\|$. For a $\mathbb{R}$ vector, an $L_2-norm$ , is the sum of the squares of the elements of that vector.

Where an area of ice has the same temperature through its depth (isothermal) then the above can be directly integrated to give;

$$u(z) \;\;=\;\; u(h^B) - \frac{2A(\bar{T}^I)}{n+1}\left(\rho^I g\right)^n\,\|\partial_j h^I\|^{n-1}\,\frac{\partial h^I}{\partial x_1}\left[(h^I - z)^{n+1} - H^{n+1}\right], \tag{2.11}$$

$$v(z) \;\;=\;\; v(h^B) - \frac{2A(\bar{T}^I)}{n+1}\left(\rho^I g\right)^n\,\|\partial_j h^I\|^{n-1}\,\frac{\partial h^I}{\partial x_2}\left[(h^I - z)^{n+1} - H^{n+1}\right]. \tag{2.12}$$

A second integration gives the thermomechanical and isothermal ice sheet fluxes respectively,

$$
\begin{aligned}
\bar{u}H &= u(h^B)H - 2(\rho^I g)^n \, \|\partial_j h^I\|^{n-1} \, \frac{\partial h^I}{\partial x_1} \int_{h^B}^{h^I} \int_{h_B}^{z} A(T^I)(h^I - z')^n dz' dz, \\
\bar{v}H &= v(h^B)H - 2(\rho^I g)^n \, \|\partial_j h^I\|^{n-1} \, \frac{\partial h^I}{\partial x_2} \int_{h^B}^{h^I} \int_{h_B}^{z} A(T^I)(h^I - z')^n dz' dz, \quad (2.13)
\end{aligned}
$$

and

$$
\begin{aligned}
\bar{u}H &= u(h^B)H + \frac{2A(\bar{T}^I)}{n+2} \left(\rho^I g\right)^n \, \|\partial_j h^I\|^{n-1} \, \frac{\partial h^I}{\partial x_1} H^{n+2}, \\
v(z) &= v(h^B) + \frac{2A(\bar{T}^I)}{n+2} \left(\rho^I g\right)^n \, \|\partial_j h^I\|^{n-1} \, \frac{\partial h^I}{\partial x_2} H^{n+2}. \quad (2.14)
\end{aligned}
$$

A non-linear diffusion equation, which can be solved for ice sheet thickness, then results from applying equations (2.14) and (2.14) to equation (2.3), known as the "ice-sheet equation" (Hindmarsh and Payne, 1996).

The basal boundary condition may contain small amounts of motion, as investigated by Payne, Het al. (2000), but "it is inconsistent with the theoretical approximations to allow these to be the dominant deformations" (Marshall, manual, p6). Marshall goes onto point out that there are also poor descriptions of the subglacial processes, and that the combination of these factors makes most of the sliding laws used in parameterisation of large-scale basal motion somewhat dubious.

### 2.3.2 Stream Flow

There are two varieties of basal interaction, known as sliding and bed-deformation. Both cases tend to be associated with liquid at the base, and in glaciers are thought to be the cause of surges– periods of much more rapid advancement of a glacier's front. Their small size and the lateral boundaries on them – created by surrounding valleys - mean that these periods of rapid advancement tend to affect the whole glacier. Ice sheets however are not limited by these lateral boundaries and are sufficiently large to make rapid flow of the entire sheet impractical. Instead fast flowing areas of ice, known as ice streams are observed to co-exist within the larger, slower ice sheet. In both cases basal interactions are the cause of the much greater ice velocities.

Generally at the base of ice masses there is some water, which will soak into the bedrock. This may be immediately absorbed into the bedrock, in which case we would think of this an ice-mass frozen to its bed. Where this bedrock is solid however, the water will not be absorbed,
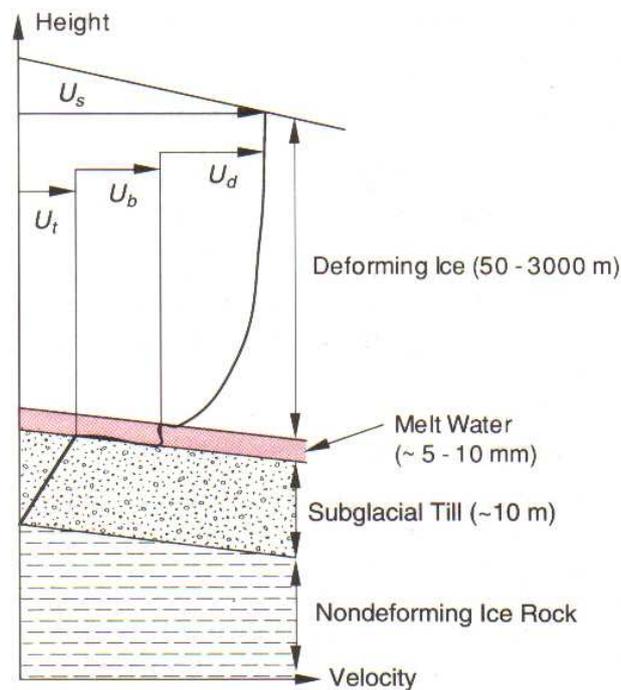
and instead will form a layer between ice and rock. This decouples the ice mass from its bed, and reduces the basal drag massively. This allows for greater ice flux, which may cause greater basal friction, and the temperature rise in turn generates more water from melting. Where the bedrock is not solid, but not all the water is absorbed, the lowered friction generated by the water causes some increase in ice motion. It also causes some deforming of the bed and it this that causes glacial till and moraines. The physical processes involved are examined in greater depth in Patterson (1994, chapters 7 & 8), and are illustrated in Figure 2.3.2.

When modelling ice stream flow the shallow ice equations become insufficient, as the longitudinal and transverse stresses become more influential than the vertical stresses. Alternatives to the shallow ice approximation have been used by Pattyn (2003), Saito et al. (2003) and Marshall (1999). Pattyn and Saito retain the longitudinal and transverse stresses in a so-called "higher-order" model, solving using the force-balance equations in their derivative, elliptic form, following the method in an earlier Pattyn paper (2000).

Marshall's approach is based on MacAyeal (1989), in which ice shelf flow was described using the reduced momentum equations, and Marshall applies this with a basal shear stress. Effectively there is no vertical shear deformation in this case, and he has to solve for ice sheet and ice stream flow separately. To do so Marshall uses continuum mixture theory, in which he

introduces a parameter $\alpha(\lambda, \theta, t)$, which is the areal fraction of ice streams in a control area. The equations for thickness, ice temperature and velocity are computed on the separate areas. Evolution of the ice streams is then computed. It occurs either by creep exchange, where ice streams feed off the sheet ice, or bed exchange, where ice streams are affected by subglacial processes.

Stream ice flow is not a dominating factor in glacier movement. Inclusion of it may well lead to improved skill in modelling individual glaciers, and certainly has value in ice sheets. However, the limited resolution at which we will be operating, and our focus on glacier modelling means that stream ice flow is unimportant here, and as such the detail of the equations are omitted.

### 2.3.3   The Effects of Dynamics

It is perhaps worth noting that not all ice-mass models consider dynamics. The IPCC compiled a best estimate of sea level rise for the 2001 assessment. To do so, they used models that were based purely on mass balance computations, which outputted the mass balance change for a given temperature and precipitation change. This is a static response, now we examine the dynamical response.

Consider a small temperature increase, so that a previously balanced glacier starts to retreat. As the lowest ice extent moves uphill, the air cools at the adiabatic lapse rate ($7.50\,^\circ$), and the surface area available for ablation decreases. The glacier will slow down its melting and retreat, and come into a new balance. The measure of this on a glacier-scale is known as the equilibrium line altitude, as shown in Figure 1.1; it represents the balance point; net accumulation occurs above it, and net ablation below it. As the glacier retreats its ELA moved upwards.

Break that process down again; firstly there is the retreat uphill, with the inherent cooling and subsequent reduction in ablation. A non-dynamical mass balance model will tell you that for a 1 degree temperature rise there will be a specific amount of mass ablated, and more importantly that the glacier will continue to ablate at that amount, until it runs of out of ice.

Secondly there is the reduction of surface area. As a glacier decreases in volume, it also decreases in surface area, and most of this decrease will happen in the area with greatest ablation. Ablation can only occur at the surface and the base, and in glaciers the surface is by far the predominant term (Patterson). Thus a decrease in surface area leads to a decrease in the rate of ablation.

The temporal evolution of the rate of ablation, and the consequential ability to model the stabilisation of a currently retreating glacier, are only possible with the use of a dynamical model. As part of their mass balance modelling Van der Wal and Wil (2001) used a parameterisation of,

$$\text{volume} \propto \text{area}^C,$$

based on work by Meier & Bahr (1996), Bahr et al. (1997) to reduce area, and this does improve the skill[3] in modelling ablation rates, but not in modelling the post-warming stabilization of glaciers.

## 2.4   Temperature Evolution and its Consequential Feedbacks

### 2.4.1   Thermodynamics

The temperature (T) of an ice sheet is not isothermal everywhere. Jenssen's approach (1977) to finding the ice temperature spatial and temporal evolution, which has been used by Huybrechts (1990) and others within the European school of modelling, is to assume that horizontal heat diffusion is negligible. Then ice sheet temperatures are given by,

$$\frac{\partial T}{\partial t} \;=\; \underbrace{\frac{k}{\rho c_p}\frac{\partial^2 T}{\partial z^2}}_{\text{vertical diffusion}} \;-\; \underbrace{U.\bigtriangledown T}_{\text{horizontal advection}}$$
$$-\; \underbrace{w\frac{\partial T}{\partial z}}_{\text{vertical advection}} \;-\; \underbrace{\frac{g(s-z)}{c}\bigtriangledown s.\frac{\partial U}{\partial z}}_{\text{dissipation}}, \tag{2.15}$$

where $k$ is the conductivity, $\rho$ is the density of ice, $c_p$ is the specific heat capacity of ice, and $w$ is the vertical velocity.

### 2.4.2   Thermomechanical Coupling

Consider the equations we have introduced thus far; thickness is a function of ice velocity, and ice velocity is a function of ice temperature, but ice temperature is also a function of ice velocity. The dissipation term in the ice-temperature evolution links it to ice flow, whilst the Arrhenius equation links ice flow back to ice temperature.

---

[3]Modellers use the word skill when referring to a measure of the level of ability with which a model performs.
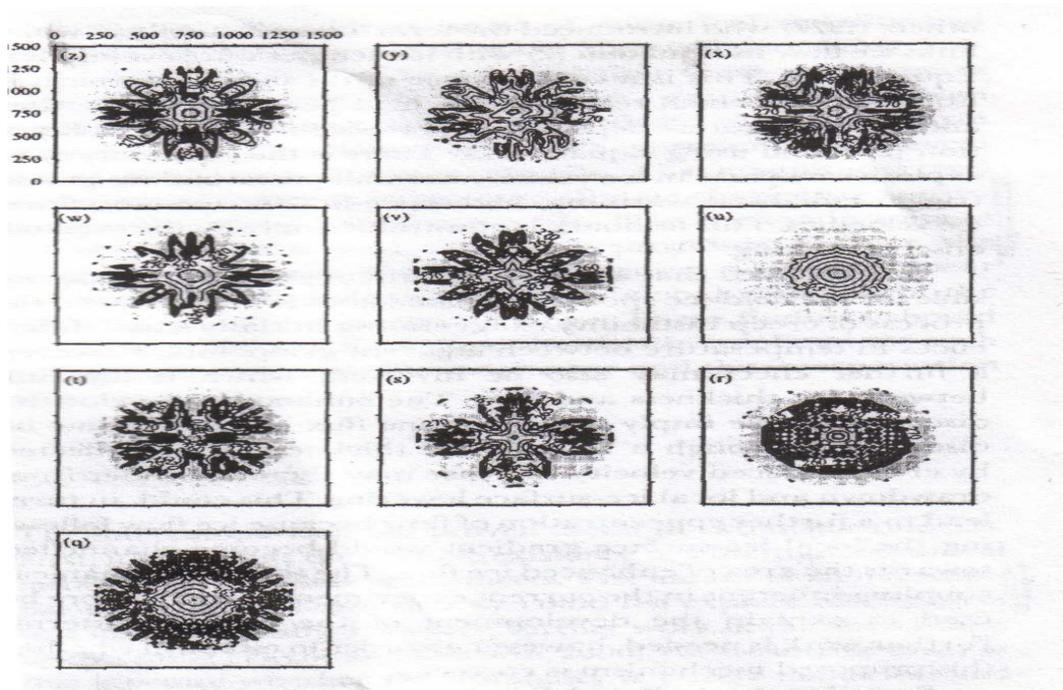
Figure 2.2: from Payne,Huybrechts et al., 2000

As part of the European Ice Sheet Modelling Initiative (EISMINT) Payne et al. (2000) examined the effects of allowing these two equations to evolve dependently. They took ten different models, using a variety of numerical schemes, but with the same core equations and working on the same grid. By applying radially symmetric climate forcings and boundary conditions, the resultant ice sheets should have radial symmetry. Payne et al. found that the thermomechanical coupling generated instabilities in the modelled ice flow, that were most apparent in the basal temperatures,(see Figure 2.2) but also seen in the ice velocity and flow-factor fields. These then lead to local changes in ice thickness and surface elevation. Payne and Donglemans (1997) encountered similar behaviour when using a rectangular ice sheet.

Clarke and others (1977) introduced the term "creep instability" to describe the link between the two equations, and noted that there is the possibility of a huge increase in velocity as a small perturbation in velocity causes enhanced warming, which causes higher Arrhenius factors, and in turn causes faster ice flow. This process is limited by the onset of melting. In fact Patterson (1994, p86) points out that above $-10\,^{\circ}C$ the Arrhenius equation does not hold, as the effective value of Q for polycrystalline ice is no longer constant.

Payne speculates that there may be another factor also causing the effects seen in Figure 2.2 - the coupling between thickness and flow. As ice velocities increase, the same flux of ice can fit through a smaller thickness, thus surface elevation falls. However, ice on the surface follows the surface, rather the topographic, gradients. Thus it will move towards the lower surface of the fast flow, and help to increase the velocity further.

At present it is still not certain that the results of the EISMINT study do reflect real processes and are not due to numerics or the simplified geometry utilised.

# Chapter 3

# Model Parameterisation Schemes

Chapter 2 showed that inclusion of dynamics is important to improving the skill in modelling ice masses. However, dynamical models have not been used in global glacier studies before. This is because the climatological and topographic data required for a global model lacks the necessary spatial resolution for individual glaciers.

This chapter examines the consequences of a lack of spatial resolution and illustrates a method for improving this as well as explaining the degree-day scheme 3.2 that is used to calculate the mass balance.

## 3.1 Nucleation within Ice Sheet Models

Inception means the development of any ice, from a blank starting field, whereas nucleation refers to the early development of an ice mass; this could occur from nothing, but is more likely to involve the evolution from small, existing glaciers.

Consider a glacier in balance, located in a region of high relief, and apply a climatic perturbation such as a period of increased precipitation or lower temperatures. This encourages the glacier to extend downwards, and in doing so it may cause feedbacks.

An increase in surface area has an associated decrease in surface temperatures, due to the albedo effect (section 2.1). As ice piles up in the valley it raises the surface height, and the increased elevation lowers surface temperatures further. A decrease in ice-surface temperature will lead to an increase in katabatic winds, which flow down glaciers and ice sheets when air is cooled sufficiently, and these will decrease the surface temperature at lower elevations.
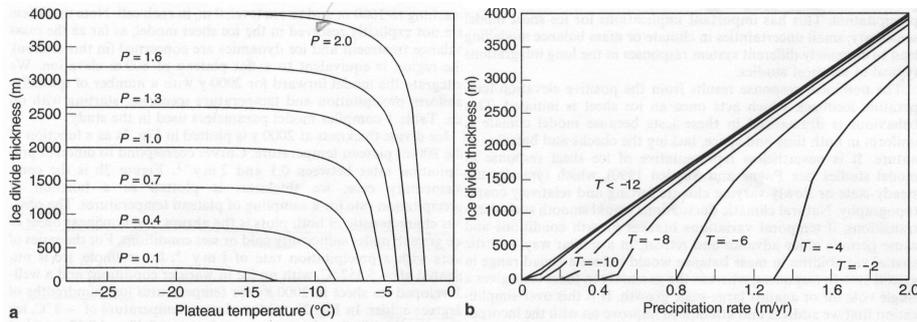
Figure 3.1: from Marshall, (1999). T is the plateau temperature ($°C$), P is the precipitation rate ($m\,a^{-1}$).

Counteracting these are the increased melt rates, associated with the glaciers increased surface area and also an increase of temperature at lower elevations. The end result could be that (1) the glacier encounters increased ablation at low altitudes sufficient to stop its growth and thus it reaches a new equilibrium, albeit at a larger size. Alternatively (2) the climatic change may have been large enough for the glacier to reach the lowest elevations of a valley, in which case the ablation rate at the lower altitudes will fall as the glaciers surface rises. The glacier then completely fills the valley, forms an ice cap, and will find other valleys into which it can flow and ablate.

In this high relief case there is almost always ice there in some quantity; changes in temperature will affect the size of the glacier in a smooth continuous way, until scenario (2) is attained. Now consider the same perturbation applied to a plateau (3); as soon as some ice develops all the positive feedbacks apply, and it will grow to be a glacier or ice cap very rapidly. Imagine lowering the temperature slowly; at the start there is no ice as temperatures melt any snow that may fall. With the decrease in temperature the percentage of precipitation to fall as snow increases and the melt rate decreases. As soon as snowfall is greater than melting the ice builds up; there is no increase in temperature at low elevations because the ice is already at a low elevation.

Thus glacier and ice sheet growth and nucleation is very dependent upon topography. In the scenarios presented the high relief terrain and plateau could easily have the same mean altitude if considered within large enough grid boxes.

Figure 3.1 shows the effects on ice thickness, for a given temperature or precipitation scenario, of varying precipitation or temperature respectively. Figure 3.1a shows that for $1.0m\,a^{-1}$ of

precipitation, a decrease in temperature from $-5.342\,^\circ$ by just hundredths of a degree is sufficient to move from the first signs of ice to a $2000\,m$ thick ice sheet. Similar non-linear sensitivity to the climatology is visible in the precipitation; for $-8\,^\circ$ an increase from $0.48\,m\,a^{-1}$ to $0.49\,m\,a^{-1}$ is all is needed. The consequences of this are that a small error in the climate data will have a very large effect on ice development. In reality mass balance varies spatially, and climatic conditions vary temporally, so that the onset of nucleation would not occur so abruptly.

Ice sheet models have been run as fine as $20-25\,km$ (Huybrechts, 1996) but are limited by the resolution of the climatological data that is used. In global models the grid cells are $\sim 100km$, at which scale individual valleys, and peaks are not resolved, and whole mountain ranges may be represented by only a few grid points (Alps, Pyrenees). The ice sheet models either miss the accumulation at high-elevations or fail to account for low-elevation ablation, which affects the generation of ice sheets in the correct places (Rind et al 1989, Marshall and Oglesby 1994).

Marshall and Clarke (1999) suggest that it is this lack of topographic detail that causes the lack of realism in studies of the growth and decay of past ice sheets. They developed a parameterisation that captures some of the subgrid topographic detail to improve the quality of inception modelling. However, by improving the treatment of accumulation and ablation they make it possible for the first time for an ice sheet model to be used on a global scale for glacier modelling.

The details are left to section 3.3 but the key is that an improvement to current ice sheet models can be made by improving estimations of mass balance on a subgrid scale. The improvements are visible in Figure 3.2, which shows the model results (Marshall and Clarke, 1999) from runs for North America, with and without the subgrid hypsometric parameterisation, compared to the present distribution of ice.

## 3.2   The Degree Day Parameterisation

Parameterisations are approximations that are used for three cases: (i) for processes that are too complex to be modelled, (ii) for processes that occur at subgrid scale so cannot be resolved but are important at grid scale and (iii) for processes that are not understood well enough to be modelled explicitly and so have to be represented empirically. An ideal model would work at a scale that includes every valley and mountain, since these will affect the growth and movement
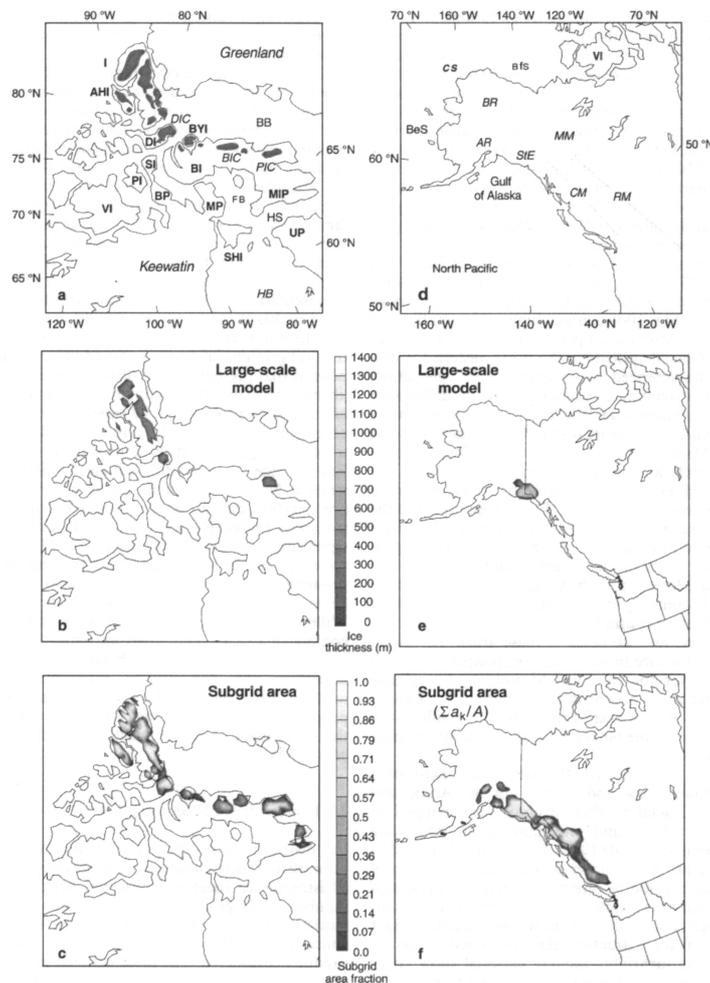
Figure 3.2: Marshall and Clarke (1999); Top row is the Canadian Arctic, bottom is the North American Cordillera. The 1st column shows present day ice, the 2nd shows the large scale model's ice thickness output, and the 3rd shows areal coverage with the subgrid parameterisation.

of ice sheets, but this is not possible as the level of accuracy required would be too expensive to compute.

As mentioned on page 14 the degree-day treatment is one of the temperature index methods, which parameterises ablation rates and the fraction of precipitation to fall as snowfall as functions of temperature. This is a well established parameterisation (Braithwaite 1984, 1995; Reeh 1991; Jôhannesson et al. 1995) that works with both annual and monthly data.

To accurately model glaciers however, annual data is insufficient. Zuo and Oerlemans (1997) showed that use of annual global averages rather than regional temperatures, and separate summer and non-summer temperatures can lead to up to a 55% difference in estimations of sea

level rise. Consider that a glacier will generally have net accumulation over the winter, and net ablation over the summer. The winter temperatures are generally sufficiently cold that a slight increase will not cause melting, whereas glaciers are much more sensitive to temperature increases during the summer months, since these directly increase melt rates. The season length also changes regionally; some glaciers will experience a longer summer melt season.

The UBC model has been written with both annual and monthly versions of the parameterisations, but we will only be using the monthly mean version, following Jôhannesson et al. (1995) and thus this is the method highlighted here.

The daily temperatures within a month are assumed to be distributed normally, with standard deviation $\sigma$. The precipitation upon a glacier at a particular altitude is assumed to fall as snow once below a threshold, usually taken to be $1\,^{\circ}C$. The fraction $f_{snow}$ of the precipitation that falls as snow in a given month is given by,

$$f_{snow} = \frac{1}{\sigma\sqrt{2\pi}} \int_{-\infty}^{T_s} \exp^{-(T-T_m^2)/(2\sigma^2)} dT, \tag{3.1}$$

where $T_s$ is the rain/snow threshold temperature and $T_m$ is the monthly mean temperature. Given volumetric precipitation rate $P(\lambda, \theta, t)$, ice accumulation is given by,

$$\dot{a}(\lambda, \theta, t) = f_{snow} P(\lambda, \theta, t) \frac{\rho^w}{\rho^I}, \tag{3.2}$$

where $\rho^w/\rho^I$ converts the snow, of density the same as water, to ice, which has a lower density. This gives the accumulation on the glacier in a given month.

The ablation, of snow and ice, is similarly parameterised as a function of the number of positive degree days ($PDD$), which are calculated from,

$$PDD = \frac{365/12}{\sigma\sqrt{2\pi}} \int_0^\infty T \exp^{-(T-T_m)^2/(2\sigma)^2)} dT, \tag{3.3}$$

where the number of days in each month is set to be equal for simplicity. The heating from the positive degree days is first directed toward the melting of new snow, as it is in reality. The degree-day factor for snow, $d_{snow}$ is different from that for ice, in part because they have different albedos. This means they absorb radiation differently and thus will melt differently.

The melt-rate of snow is given by,

$$\dot{m}_{snow}(\lambda, \theta, t) = d_{snow} PDD(\lambda, \theta, t)(1 - r_f), \tag{3.4}$$

where $r_f$, the refreezing factor, accounts for water that melted but then refroze rather than running-off.

Ice ablation is then the result of any surplus heat energy after the snow has been melted. It is calculated from the number of surplus $PDD$s,

$$\dot{m}_{ice}(d) = d_{ice} \left( PDD - \frac{\dot{m}_{snow}}{d_{snow}(1 - r_f)} \right) (1 - r_f). \tag{3.5}$$

The mass balance is then the accumulation (equation (3.2)) plus any ice flux, minus the ablation (equations (3.4) and (3.5)).

## 3.3   The Subgrid Hypsometric Parameterisation

### 3.3.1   Motivation

Hypsometry is the distribution of the elevation of land above sea level; it is a way of quantifying the phrases "high relief and "plateau. Table 3.1 shows the difference between the mean grid cell elevation and the maximum and minimum elevations within cells in the Himalayas taken along a line of latitude $(35\,^{\circ}N)$ [1]. It is a good example of how entire mountain ranges become smoothed away by the large-scale averages taken over a grid box and highlights the importance of incorporating the subgrid topographic detail in some way in order to improve mass balance modelling, and thus allow an ice sheet model to produce glaciers. The Himalayas are especially hard to model in an ice sheet model due to their relatively low latitude ($\sim 35\,^{\circ}N$) and high relief; when the mean elevation is used they are too warm to develop ice.

Whilst it would be impractical to attempt to model on the scale of individual valleys and peaks, the data from within the grid cells can still be used to improve the model.

---

[1]from the etopo2 dataset, see Chapter 5

| Longitude | 71.25 $^\circ E$ | 75 $^\circ E$ | 78.75 $^\circ E$ | 82.5 $^\circ E$ | 86.25 $^\circ E$ | 90 $^\circ E$ | 93.75 $^\circ E$ |
|---|---|---|---|---|---|---|---|
| Maximum(m) | 6330 | 8311 | 6970 | 7010 | 6184 | 6480 | 6055 |
| Mean(m) | 2388 | 3657 | 5158 | 5133 | 5063 | 5026 | 4629 |
| Minimum(m) | 253 | 513 | 2466 | 2406 | 4705 | 4012 | 3032 |

Table 3.1: Differences between mean, max and min cell heights in the Himalayas along a constant line of latitude ($35\,^\circ N$)

### 3.3.2  Derivation of the Hypsometric Curve

Suppose the range within a grid cell is split into $n_h$ levels evenly distributed across the heights, with the lowest elevation labelled bin 1. Then compute how much area within a grid cell is at each elevation. This is illustrated in Figure 3.3, where the graphs show the distribution of area with elevation within a grid cell. Then calculations of accumulation, ablation and ice flux can be performed on each bin. Whilst the valleys geographical details are lost, the concept of ice accumulating at altitude in the highest bins and flowing downhill to be ablated in the lower bins, as described earlier, is maintained and this should improve model accuracy.

Digital Elevation Modelled (DEM) data on a subgrid scale could be used to calculate the area at each level, but to do this on a large scale is very costly[2] and some regions are not publicly available as yet. Marshall and Clarke used Row and Hastings' (1994) DEM data at 30-arc sec resolution to compile hypsometric curves for various types of terrain – rugged mountainous, gentle prairie and plateaus to name a few.

The important difference between regions is the spread of their subgrid hypsometry; the Alps and Himalayas will act similarly despite having different means and ranges of elevations because they are the same type of terrain. To remove the issue of means and ranges they normalize, which is where all the data is adjusted so that its lowest elevation corresponds to zero, and its highest to 1. They then observed that the normalized hypsometric curves of cell relief, shown in Figure 3.3, all have a similar shape, and so belong to a similar topological family.

By generating a synthetic hypsometric curve which gives a good fit to each scenario they found they could conserve the hypsometric properties of a region without having to find and carry the subgrid DEM data.

Firstly they normalize by cell relief, $\triangle h^B = h^B_{max} - h^B_{min}$, where $h^B_{max}$ and $h^B_{min}$ are the maximum and minimum heights of the bed topography. The normalisation returns a unit

---

[2]Marshall and Clarke (1999) estimate that using 30-arcsec data would require 311mb of memory per $1\,^\circ$ cell
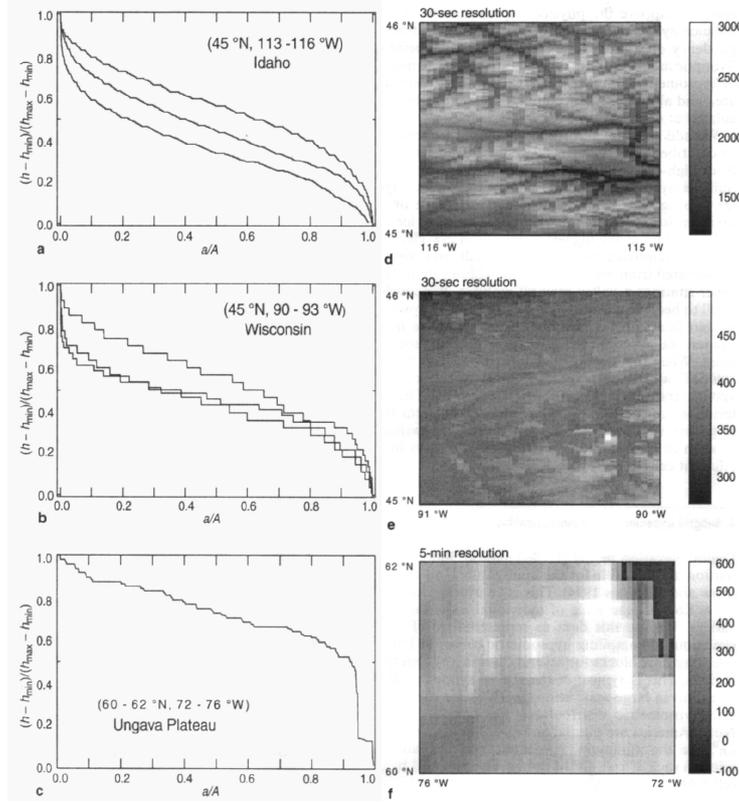
Figure 3.3: from Marshall and Clarke (1999)

mapping,

$$\frac{h^B - h^B_{min}}{h^B_{max} - h^B_{min}} = f(a/A), \tag{3.6}$$

where $A$ is the grid cell area and $a/A$ represents the cumulative subgrid area above elevation $h^B$. The synthetic hypsometry curve used is then given by,

$$
\begin{aligned}
\hat{h} &= \frac{h^B - h^B_{min}}{h^B_{max} - h^B_{min}} \\
&= \left[ \operatorname{atanh}[b(2a/A - 1)] + \frac{\operatorname{atanh}(-b)}{2\operatorname{atanh}(-b)} \right]^c.
\end{aligned}
\tag{3.7}
$$

Their choice of synthetic curve, equation (3.7), is justified on the grounds that it produces a good fit for the test data. Free parameters $b$ and $c$ control the curvature of the function and the asymmetry in the curve respectively. This allows for a variety of curves to be produced, as illustrated by Figure 3.4.

By noting that the normalized median elevation - which is halfway between the maximum
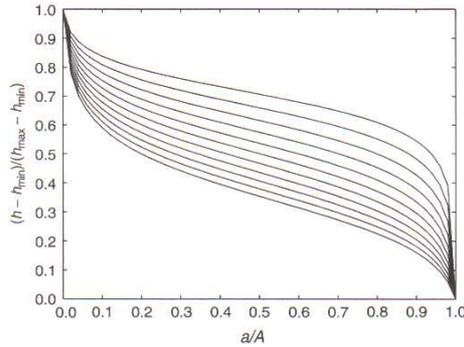
Figure 3.4: from Marshall and Clarke (1999)

and minimum - will map to point $a/A = 0.5$ a value for $c$ can be found explicitly,

$$
\begin{aligned}
\langle \hat{h} \rangle &= \frac{h^B - h^B_{min}}{h^B_{max} - h^B_{min}} \\
\Rightarrow \quad c &= \frac{\ln(\langle \hat{h} \rangle)}{\ln(0.5)}.
\end{aligned}
\tag{3.8}
$$

Marshall and Clarke (1999) were able to find a misfit minimizing value of $b = 0.977$. To do so, they calculated the misfit between the synthetic function and the real data over 500 cells, as a function of $b$, then looked for a misfit-minimising value in the range $(0.96, 0.999)$,

The regions that were presented in Figure 3.3 have their DEM data compared to their synthetic hypsometric curves in 3.5.

### 3.3.3  Applying the Parameterisation

To apply the parameterisation, the hypsometric curve of each cell must be found in order to compute the area and height of each bin within the cell. The accumulation and ablation are then calculated for each bin, and ice flux between bins is also computed.

The hypsometric curve seems complex, and in fact a linear curve could have been used and would still provide an improved representation of mass balance. However, computation of the various subgrid cell hypsometries only occurs once per model and thus the improved fit justifies the marginally higher cost. The curve is found by performing the following;

- Divide the range of elevation in a cell by the number of bins required[3] then spread the

---

[3]Marshall and Clarke (1999) found in their tests that accuracy did not improve significantly above 8 bins
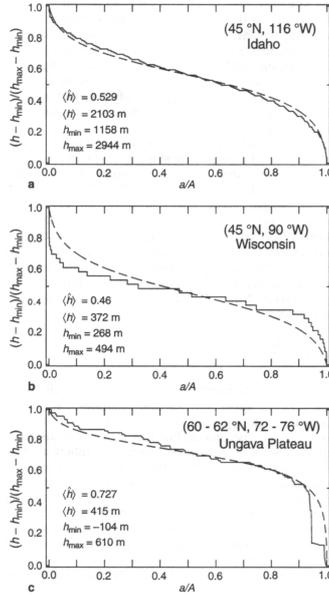
Figure 3.5: from Marshall and Clarke (1999)

elevations of the bins evenly over the range, with spacing $\triangle h$

$$h_k^B = h_{min}^B + \triangle h \left( h - \frac{1}{2} \right), k \in (1, n_h).$$  (3.9)

- A rearrangement of equation (3.7) then gives the subgrid cumulative area,

$$a/A = 1/2 + \frac{\tanh(\hat{h}^{-c} - 1/2)}{2b},$$  (3.10)

which is easily broken down into the subgrid area for each bin.

At this point, for each bin, subgrid elevations and areas have been found. Accumulation ($\dot{a}_k$) and ablation ($\dot{m}_k$) are calculated using the same degree-day parameterisation that was explained in section 3.2, but with improved temperature and precipitation estimates.

Temperatures for each bin are generated by adjusting for elevation above sea-level using the adiabatic lapse rate. This is a common feature in dynamical models because it allows them to evolve the surface temperature with changes in ice sheet thickness. However, rather than adjusting for the mean cell height the temperatures in each bin are computed based on the elevation of that bin. Assuming that the precipitation data is at surface height rather than sea level and so already shows the effects of elevation, it is spread evenly over all bins except above

a threshold known as the drying height.

This threshold is a chosen distance above the mean cell level, designed to mimic the elevation-desert effect at high altitude or when an area becomes heavily glaciated, where the air becomes very dry and thus precipitation drops off. Above this point the precipitation is reduced exponentially with height. In cases where the drying height is reached, and upper levels have their precipitation reduced, the surplus is then spread evenly over the lower levels. When modelling for North America, Marshall and Clarke (1999) chose to use 1000m as their drying height.

Marshall and Clarke (1999) recognized in their original work that the processes involved in precipitation distribution are very complex, especially so in mountainous regions, and that the details of absolute elevation, local winds and moisture sources may be more important than the simple elevation effects embodied in the drying parameter. Barry (2001) presents work by Lauscher (1976), that is repeated here in Figure 3.6, when discussing the details of precipitation lapse rates. They are noticeably different for regions of interest in this study; middle latitudes have significantly greater precipitation with height whilst polar regions have decreasing precipitation linearly with height. Barry notes that whilst Lauscher's profiles are useful generalities, the local and regional complications often outweigh these simple rules, with some mountains having different profiles on different slopes (Mt. Cameroon, Lauer (1975)) and others having seasonal fluctuations (Bavarian Alps, Erk (1887)). This indicates that Marshall and Clarkes (1999) precipitation lapse rate[4] may be incorrect when applied to a global mapping.

Accumulation and ablation have been accounted for, now dynamics need to be applied. Recall that the ice build-up on the hypsometric curve is an idealized distribution of the areal coverage of ice across the elevations within a cell, and not a picture of the true, often complex, subgrid topography and ice distribution. Thus the dynamics as described in section 2.3 cannot be applied. However, dynamics are crucial to improving the skill of the model and so a subgrid parameterisation of ice flux is used.

### 3.3.4 Subgrid Ice Flux

Figure 3.7 illustrates the concept of subgrid ice flux. At time $t^m$ the ice in bin $k$ is $H_k^m$ metres thick, giving a bin volume of $V_k^m = H_k^m a_k$. Let $Q_k^{m+1}$ be the volume flux per unit area of ice moved from subgrid bin $k$ to bin $k-1$ between time segments $t^m$ and $t^{m+1}$. The total volume

---

[4]which is probably correct for the polar regions that the model was originally intended for
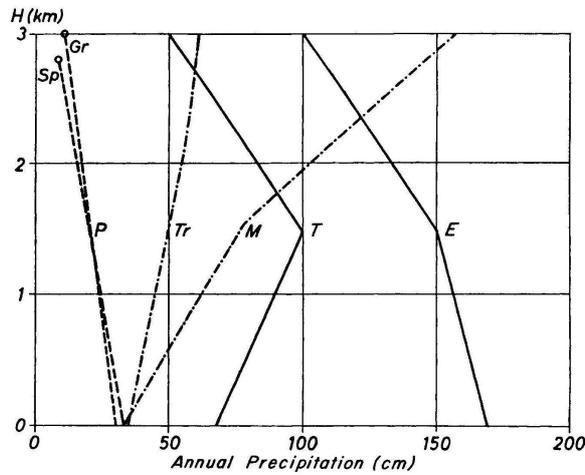
*Figure 4.13* Schematic profiles of mean annual precipitation (cm) versus altitude in
equatorial climates (E), tropical climates (T), middle latitudes (M), and polar regions (P)
*Notes*:  SP denotes Spitzbergen; Gr Greenland; Tr is a transitional pattern between latitudes
30 and 40°N
*Source*:  After Lauscher 1976a

Figure 3.6: from Barry (2001), p233
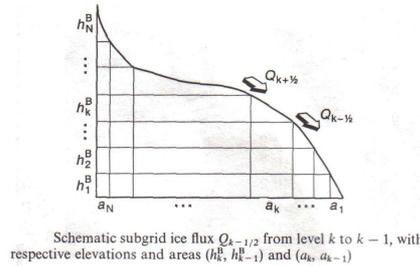


Schematic subgrid ice flux $Q_{k-1/2}$ from level $k$ to $k-1$, with
respective elevations and areas $(h_k^B, h_{k-1}^B)$ and $(a_k, a_{k-1})$

Figure 3.7: from Marshall and Clarke (1999)

flux of ice is then $a_k Q_k^{m+1}$.

Ice is assumed to be incompressible. Then for all bins except for the top (where there is no influx of ice from above) the ice thickness evolution in bin $k$ is the result of the incoming ice flux from bin $k + 1$, the outgoing ice flux from bin $k$, and the mass balance of bin $k$,

$$
\begin{aligned}
\frac{\partial H_k}{\partial t} &= \frac{a_{k+1}}{a_k} Q_{k+1} - Q_k + \dot{b}_k, \ k \in (1, n_h - 1), \\
&= -Q_k + \dot{b}_k, \ k = n_h.
\end{aligned}
\tag{3.11}
$$

The ratio in front of the incoming ice flux from bin $k+1$ represents the difference in area between the two bins. The incoming ice, of quantity flux x area of upper cell must be spread over the

area of the cell into which it flows into.

Marshall and Clarke (1999) suggest an ice transport rule that is physically based, but relatively simple. They assume ice can only move down one bin each time step, so the amount of ice within a bin that is available to move must be the product of the area of the bin with the thickness of ice within it. The thickness of ice within a subgrid bin from the previous time step is known and added to the mass balance that has occurred within that time step. This gives a total volume of ice ready for transport ready for transport at time $t^{m+1}$ of $a_k(H_k{}^m + (\dot{b})_k{}^{m+1}\triangle t)$.

The ice flux parameterisation is then a function of this volume,

$$Q_k{}^{m+1} = \frac{1}{\tau}(H_k^m + \dot{b}_k^{m+1}\triangle t)[1 - \exp(-(\triangle h_k^{I\,m}/L_k)^3)], \qquad (3.12)$$

where $H$ is ice thickness and $\triangle h_k^{I\,m}$ is the difference in elevation of the two ice surfaces ($h_k^{I\,m} - h_{k-1}^{I\,m}$), i.e. the surface slope, at time step $m$ in bin $k$.

As the time step is decreased the mass balance term goes to zero and the subgrid ice flux becomes a function of bin thickness; the more ice a bin has the more quickly it will try and flow out. This is diffusive relaxation; start with a lump of ice in the top bin of a cell, after the first time step some of the ice has moved down to the next bin, reducing the height and thus the speed at which it flows.

However, a more realistic approach should take account of the fact that the slope between bins affects how fast the ice will flow, which is what the $\triangle h_k^{I\,m}$ term does. The ice surface rather than the bed topography is used because ice flow follows the contours of the surface. Without this term, should the ice reach the bottom bin in a cell, then it will continue to pile up in just that bin. The addition of this term means that the glacier will modulate flow towards a level state. As the slope between adjacent cells decreases to nothing ($\triangle h_k^{I\,m} \to 0$), such as on a plateau or if ice at the lower levels has piled up, the flux also tends to zero.

The inclusion of each bins mass balance allows for a dynamic equilibrium to be reached, such that the rate of melting in the lower bins matches the rate of flux from the upper bins. Whilst this is perhaps not a rigourous physical argument, it does match the concept of glacier flow.

Whilst a glacier will adjust immediately to changes in its mass balance, it will not immediately reach a new equilibrium, but instead has a characteristic dynamic adjustment timescale (equation 1.1). To take account of this a time scale for flux response, $\tau$, is included in the equation and is in the order of 10 years (Marshall and Clarke, 1999).

Similar to a half-life, $L_k$ is a length scale that measures how long ice stays at one level. A first order Taylor series expansion of equation (3.12) gives $Q_k \propto H_k(\triangle h_k^I \,^m/L_k)^3$. Marshall explains that they chose an exponent of 3 in equation (3.12) because the dependence on surface slope is then similar to Glen's flow law for glacier ice (equation (2.6)),(Paterson, 1994). He goes onto suggest an appropriate form for $L_k$ in terms of cell hypsometry,

$$L_k = \frac{L_0 a_k}{A},\tag{3.13}$$

where $L_0$ is a horizontal length scale for the cell. The perimeter of the cell should not be used for $L_0$ because cell size will vary depending on (1) the chosen grid resolution and (2) on meridional position if on a spherical grid. If it were, then the flow of ice would be independent on the discretisation chosen. Marshall and Clarke (1999) suggest a constant value of $50\,km$ as suitable on their $1\,^\circ$ by $1/2\,^\circ$ grid.

### 3.3.5   Subgrid-Grid Interaction

The subgrid hypsometry could be used throughout the entire model run, but for fully glaciated regions such as Antarctica there is little to be gained since the surface is relatively flat and the cost of computing new subgrid hypsometric curves - to take account of the evolving ice sheet surface - is high. Entirely glaciated cells are already modelled relatively well; the subgrid hypsometric parameterisation will add little improvement except in areas of high-relief where subgrid effects may play a role at all times (Marshall and Clarke, (1999)). Therefore as the integration proceeds the model can choose not to use the subgrid treatment in some cells.

When a cell fulfils a given criterion it is deemed glaciated, at which point it acts as part of the large-scale system and subgrid mass balance and ice fluxes are no longer considered. Similarly, when another criterion is filled the cell is deemed to be deglaciated and subgrid processes are considered once again.

A cell may receive ice from its neighbouring cells at any stage, but it may only output ice to its neighbours when it is deemed glaciated. Within a cell the lowest bin may gain ice from (i) flux from the bin above it, (ii) from direct accumulation and (iii) input from neighbouring glacierised cells. The lowest bin often has a small area, and thus the influx of ice from neighbouring cells can be sufficient to raise the surface elevation above that of the next lowest bin. Should this

happen, the ice thicknesses are adjusted so that the bottom two cells have the same surface elevation, and if this then exceeds the ice elevation in bin 3 the levelling is extended to include that bin, etc.

Once the grid-scale incoming fluxes have been computed the subgrid mass balances are calculated. If the low-elevation ablation is not sufficient to melt all the ice that has built up in the bottom bin during that dynamic time-step then the cell is deemed to be glacierised and the subgrid processes are now ignored.

For glacierised cells there is only one value for the thickness of ice within the cell, $H$. Recall that the subgrid bins were spread evenly over the range of elevations within a cell, so that the difference in elevation between any two adjacent bins in the same cell is constant, bin-step = range/nos of bins. If $H <$ bin-step then the cell is deemed to have become deglacierised and the subgrid processes are reapplied.

The criteria and rules on interaction between cells are somewhat arbitrary, and Marshall and Clarke (1999) suggest there is room for a more sophisticated system.

## 3.4   The Grid

The ideal grid for modelling the globe would be a sphere however this introduces many numerical issues. To avoid this, the UBC ice sheet model is built on a spherical co-ordinate system $(\lambda, \theta, z)$ with decreasing grid-cell size $(\triangle\lambda, \triangle\theta, \triangle z)$ as it moves towards either pole, as with the Earth. The model was constructed to run on a limited-extent grid $(n_\lambda, n_{theta}, n_z)$, and so does not have the necessary components to deal with ice moving over the poles or around its longitude borders, i.e. off part of the grid and back on elsewhere.

When it was first developed it was envisaged that wherever one chose to model, a grid suitably large could be constructed such that the ice would not reach the boundaries, but instead would evolve to its natural $H = 0$ limits[5]. For example when Marshall and Clarke (1999) modelled North America they already had the Arctic, Atlantic and Pacific oceans as natural barriers. To be sure that there would not be any undue ice build up at the edges they took a diffusive approach; subscribing almost infinite ablation $(20m\,a^-1)$ at the two outer-most grid-points.

Problem areas are thus at the borders. Glaciers and ice caps are high latitude features but are not so significant at the extremities of north and south, where ice sheets and shelves take

---

[5]from personal correspondence with Dr Marshall

over. The data we will be using works from the Greenwich meridian eastwards. This will mean the loss of the small glaciers in France and Spain, as well as some of the Norwegian network. However, this loss is minimal, and the ice sheets at the poles are not of direct concern to this study, thus Marshall and Clarke's approach is maintained. As a sub-note, the model encounters convergence issues associated with the very small grid spacing when extending to the poles $(90\,^{\circ}N/S)$, and so we choose to run from $85\,^{\circ}N$ to $85\,^{\circ}S$.

# Chapter 4

# Design of Experiments

There are two components to consider in designing the model runs: examining the data to be used, and justifying the experiments to be run on those data.

## 4.1 The Input Data

The UBC ice sheet model requires, as a minimum, climate forcing, bed topography and initial ice thickness. However since this study will be using inception runs (section 3.1) the initial ice thickness field is unnecessary.

### 4.1.1 Bed Topography

The modelled DEM data which will be used is from etopo2[1] , and extends from $0\,°$ eastwards to $365.25\,°$, and from $90\,°N$ to $90\,°S$. However, the model has not been written to deal with the significantly narrowing cell areas and widths that occur near the poles and so the northernmost and southernmost $5\,°$ are excluded. This presents no problems since there are no mountain glaciers in these regions. Use of the non-physical boundary conditions (section 3.4) means that whilst the equations are solved on the full grid ($0\,°E - 360\,°E$ by $85\,°N - 85\,°S$), the output is only valid for $7.5\,°E - 348.75\,°E$ by $80\,°N - 80\,°S$. The resolution of the climatological data is such that it is applied on a 96*69 point grid (long*lat), with outputs on the reduced physical grid of 92*65.

---

[1]etopo2 is a product of the National Geophysical Data Center. The extensive references and methodology for the data compilation can be viewed at http://www.ngdc.noaa.gov/mgg/image/2minrelief.html

Topographic data that is required is the maximum, mean, and minimum elevations for each grid-cell, and this is computed from the etopo2 DEM data, which was provided at 2-minute resolution. The land fraction has also been calculated with the etopo2 data, and gives a subgrid representation of the land fraction of each cell. The mean elevation and land fraction are used by the model as the grid-scale bed topography. The mean elevation is also used with the maximum and minimum elevation data to generate the hypsometric curves for each grid-cell. These curves are then used to calculate subgrid bin areas and elevations.

### 4.1.2   Climate Forcing

The atmosphere and oceans are modelled separately, with the models coupled to each other through sea–surface fluxes of heat and carbon. Subgrid processes such as cloudiness and precipitation are parameterised in the atmospheric model. They are limited in their ability to model the climate [2] but they are, however, the only physically based way to calculate a regional and seasonal pattern of climate change. This is important because climate change will not be uniform and it has already been shown in this study that glaciers react differently to summer and non-summer changes.

The climatological data consists of temperature and precipitation grids. Two versions will be applied: a modelled and an observed dataset. The modelled dataset is from the 3rd version of the UK's Hadley Centre Climate Model (Gordon et al. (2000)) and is provided at a resolution of $2.5\,^{\circ}$ in the latitude, $3.75\,^{\circ}$ in the longitude. The climate model (hereafter HadCM3) is run with an atmospheric composition approximating that of 1860 for a period greater than 1kyrs, during which it is stable. The data is the result of a 100 year mean from within this period.

Most ice sheet models are designed to run on either annual or monthly climate data, the UBC model will accept either, but as was established in section 3.2 monthly data are used due to the greater accuracy. Data that can distinguish between the seasons is especially important if a model is to be used in climate change experiments, as change is most likely to be both regionally and seasonally varying (section 3.2).

HadCM3 produces surface-height temperature data, whereas the model requires sea-level temperature data. This is because it will adjust the surface temperature with surface height, which can vary due to changes in ice thickness[3]. This means that the HadCM3 data must

---

[2]see Gordon et al (2000) for details of the problems with the Met. Offices Hadley Centre model

[3]on much longer timescales, beyond the scope of this study, the ground thickness may also change, due to

be adjusted, and since the topography is dictated by etopo2 DEM data, the temperature data must be adjusted using this - warmed with decreasing height at a typical adiabatic lapse rate of $\sim 7.5\,^{\circ}C\,km^{-1}$.

Note that etopo2 and HadCM3 do not use identical pictures of the globe. Firstly they do not both include the same islands. Secondly and more crucially, HadCM3 uses an orography which is the area-average elevation within its grid cells. In coastal regions HadCM3 averages over the land and sea areas, which means that the land mean elevation in a cell is lower than we would expect. This in turn makes the surface temperature warmer than it should be over land.

When constructing the mean, maximum and minimum grid cell elevations from the Etopo2 data only the land elevation within each cell was taken consideration, giving a land-height representation as we would expect it to be. To correct for the difference in perspective between the climate data and the topographic data a correction was applied to the HadCM3 data.

The observed climatological data comes from the Climate Research Unit (New et al. (1999)) at the University of East Anglia. The dataset[4] (herafter CRU) is the result of interpolating all station data in the period 1961-1990 to a resolution of $0.5\,^{\circ}$ which has then been area-interpolated to the resolution required for these model runs. Note the newer period means that these datasets are not directly comparable, and a slight warming may be expected in the CRU set relative to the HadCM3 dataset. The CRU data does not cover the oceans or Antarctica, and its temperatures also have to be adjusted to sea level, but it should offer more accurate data at the coastline, since it was taken nearer the height etopo2 expects the land to be.

The perturbations to the climate are computed in line with a 4x $CO_2$ rise ($\sim 1080ppm$) which is at the upper end of the stabilisation levels considered by the IPCC, but is a standard scenario for climate modelling. The HadCM3 model was run for 300 years (from present), and whilst the model climate has not reached an equilibrium state by this point, the rates of change are sufficiently small so as to be considered converged. A 30-year mean of the 4x $C0_2$ climate is used to produce the monthly mean temperature and precipitation fields.

---

isostasy and tectonic plate shifts

[4]raw data available from http://ipcc-ddc.cru.uea.ac.uk

## 4.2 Experiments Undertaken

The experiments fall into three broad categories; implications of the hypsometric parameterisation, equilibrium runs, and climate change scenarios.

### 4.2.1 The Hypsometric Parameterisation

The model allows for the hypsometric parameterisation not to be applied. This means the effects of the parameterisation can be examined, by quantitative comparisons of the total ice volume and total areal coverage, and qualitative analysis of the areal coverage. Qualitative analysis of areal coverage involves examining plots of the areal coverage to see if the separate model runs produce ice in the same areas, and more importantly if the parameterisation improves the skill of the model. This can be measured by comparing the output to the current spread of ice across the globe. To do so would be to reproduce, and thus reinforce, a result Marshall and Clarke (1999) found when modelling the North American continent.

Examining the subgrid ice thickness in a variety of bins at a limited number of specific locations shows if the model is distributing the ice across the heights appropriately. Moreover, choosing suitable locations that have distinct hypsometries whilst similar mean altitudes will test another of Marshall and Clarke's results; that distinct hypsometries produce distinct ice-masses.

### 4.2.2 Control Runs

These runs use the subgrid hypsometry, and test to see if the model will produce a stable and realistic state for glaciers. They will be 1500 year runs, which are too short to properly develop ice sheets, but should give glaciers and ice caps sufficient time to develop. Most glaciers have dynamic adjustment timescales in the range 10-100 years, whilst ice caps are a little slower, nearer the 800-1000 year mark. We test for convergence to an equilibrium level by examining a time series of total areal coverage and total volume.

Should an equilibrium be reached, use of the two different datasets, in combination with regionalised glacier volume data[5](see Figure 4.1) will allow for a comparison of the modelled volumes with observationally based inventories.

---

[5]Zuo and Oerlemans dataset, with Van der Wal and Wils data for Greenland
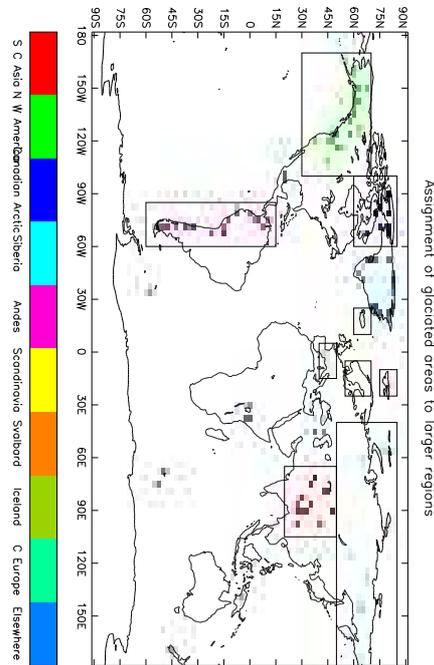
Figure 4.1: Regional datasets used in glacier volume comparison

### 4.2.3   Climate Change Scenarios

The first climate change experiments are simple adjustments made uniformly across the grid, in which the effects of adjusting the temperature field by 1 degree are examined. Figure 9.18 and Table 9.4 in the IPCC TAR suggest that an increase of 1 degree in the global average temperature is accompanied by an increase of approximately 2% in the precipitation levels. For this reason the entire precipitation field will be increased by 2% appropriately.

In addition to the standard climate change run, tests with changes applied to only one of the climatic fields should allow the fields to be prioritised in terms of their effects on glacier mass balance. Moreover, tests with twice the warming and with the perturbation applied as a cooling will examine whether these changes are linear, and symmetric.

Gregory and Oerlemans (1998) and Zuo and Oerlemans (1997) show considering changes in the summer melt season and the rest of the year separately is necessary for accurate modelling of glacier response to climate change. This is because most glaciers are particularly sensitive to melt-season warming. In general the uniform warming will produce more ablation since it warms as much in summer as winter, whereas climate change is temporally biased towards the

winter season.

Such simple climate changes are not likely to represent the genuine climate change, but they are significantly easier to comprehend. They aid the understanding of how glaciers on a global scale will react to climate change, and their sensitivity to some of the main factors involved.

The next set of experiments are performed using the HadCM3 predictions for future warming under the 4x $C0_2$ scenario. The HadCM3 predicted data can be run directly. To apply the perturbations to the observed data requires a more complex, but quite commonly used method. The temperature field is raised by adding the perturbation in the HadCM3 data, whereas the precipitation field is adjusted by multiplying by the fractional change,

$$\text{fractional change} = \frac{\text{perturbation data}}{\text{original data}}. \tag{4.1}$$

The reasons that justify this approach are: firstly the precipitation field is positive definite, whereas the temperature field is not; and secondly that precipitation tends to increase by a constant ratio for a given increase in temperature.

Temperature and precipitation vary regionally under climate change projections; Figures D.2 and D.2 in Appendix D show the differences in temperature and precipitation patterns between the 1860-climate run and the $4xCO_2$ scenario.

Both sets of climate change experiments will have their ice volume loss calculated from the equilibrium values found earlier, and thus a contribution to sea level rise can be computed.

# Chapter 5

# Results

As explained in chapter 5 there are three classes of experiments considered in this study. The results of the control experiments for the HadCM3 and CRU datasets are considered first as these will be used as a benchmark in the other tests. Throughout this chapter figures are constructed such that the HadCM3 run is shown in (a) and the CRU results in (b), unless otherwise noted.

## 5.1   Control Runs

The first consideration with the model is whether it develops a stable state. The totals of volume for the two datasets are shown in Figures 5.1(a) and (b). The total global ice volume, inclusive of the ice sheets is shown in 5.1(a).

The ice sheets take much longer to equilibrate with their climate because of their longer timescale for dynamic adjustment (see section 1.4), and have much greater volumes. This explains why the curves in Figure 5.1(a) show no sign of stabilising. The lack of Antarctica in the CRU dataset partly explains why there is less total ice volume.

Figure 5.1(b) shows that in both runs glacier volume converges. Noting the difference in scale, the HadCM3 run has greater glacier volume because the mountainous areas have a slightly colder and wetter climate. The climatological differences in the datasets are illustrated in Figure 5.2.

Convergence of glacier volumes implies that the glaciers have reached a stable state, which is a prerequisite for the modelling in this study. It is important however, to know whether this stabilised state is realistic. Consideration can first be given to the areal coverage of glaciers as shown in Figures 5.3(a) and (b). These show the fraction of each grid-cell that is covered with
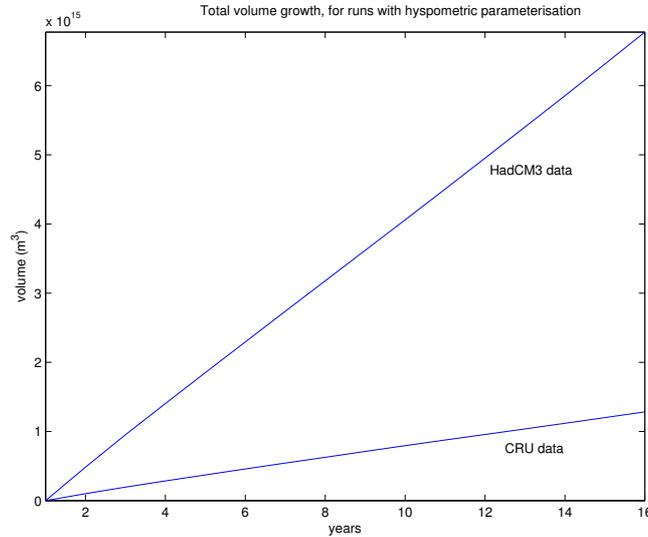
Figure 5.1: Plots of the variation in total global ice volume with time, for the control runs. (a) is inclusive of the ice sheets, but the CRU dataset does not include Antarctica, and (b) is the result of excluding the ice sheets.

ice, and on a large scale are directly comparable with Figure 4.1 and most world maps. The large features of Greenland and Antartica are immediately visible, as are the Himalayas and the North American Cordillera.

A more quantitative approach can be achieved by comparing the global glacier area and volume totals to observationally based estimates[1]. The global glacier sea level rise($SLR$) equivalent, which means how much sea level would rise if all the glaciers were to melt entirely, can be calculated by,

$$\text{Volume}_{SLR} = \frac{\rho_{ice}}{\rho ice} \quad \frac{\text{total glacier volume}}{\text{surface area of the oceans}} \,, \tag{5.1}$$

where the surface area of the oceans is taken to be $3.62 \times 10^{14} \, m^2$. The results are presented in Table 5.1. Of note is that the HadCM3 data causes a significant overestimation of area. Most of this is coming from one grid cell in Alaska, which has substantially more ice volume and ice areal coverage than it should. This may be attributable to excessive precipitation in that region. As well as the Alaskan cell there is also an over-estimate of the ice levels on Kerguelen, an island in the south of the Indian Ocean. Removal of these two points in the HadCM3 data leads to the column "improved" estimates in Table 5.1.

The CRU model seems to estimate the area well, but under-estimates the volume, whilst

---

[1]Zuo and Oerlemans data, supplemented with Van der Wal and Wild for Greenland

|  | Estimate | CRU | HadCM3 | Improved |
|---|---|---|---|---|
| Ice Area ($10^6 \, km^2$) | 0.598 | 0.4 | 2.3 | 0.99 |
| Ice Volume ($10^6 \, km^3$) | 0.218 | 0.165 | 0.315 | 0.24 |
| SLR equivalent ($m$) | 0.603 | 0.052 | 0.998 | 0.68 |

Table 5.1: Comparison of the volume and area totals produced by the model, under the two datasets, to the totals from an observationally based dataset.

the HadCM3 model gives better results for volume, but over-estimates the area. This tendency can also be seen across most regions, Appended Figures C(a) and (b)illustrate regional volumes (without the corrections) where it is clear that the global trend is repeated in most regions. This suggests that it is either a global-scale error in the climatological data or in the way the model handles that data, rather than a regional anomaly. The nature of the error suggests that the problem lies in the relationship of volume–to–area in the model; specifically that there is too little volume for a given area, which would mean that the glacier ice is not thick enough.

Alternatively, the volume–to–area relationship used in constructing the inventory may be in error. The model uses a simpler, degree–day scheme, whereas Oerlemans used an EBM which is more accurate but was based on data for only a few glaciers and then extrapolated to the world. In doing so they assumed that the glaciers they used represented the entire world accurately. Thus it is not clear which volumetoarea relationship is correct.

## 5.2 Effects of the Subgrid Hypsometric Parameterisation

The control runs calculated in the previous section are now compared to model runs that have not used the subgrid hypsometric parameterisation. The difference between the two, in terms of the fraction of a grid cell that is covered in ice, is shown in Figure 5.4

The values seem small but this is because of the large scale of the grid cells which, at the equator, can be as large as $100,000 \, km62$. More importantly, the sum of the area of glaciers and ice caps was shown in the previous section to be of the right order of magnitude whereas when the subgrid hypsometric parameterisation is switched off the model produces no ice at all except over the ice sheets. This shows that the subgrid hypsometric parameterisation allows an ice sheet model to develop glaciers.

The next consideration is that of how the parameterisation is distributing ice over the subgrid bins. An examination of the mean heights of cells in the Himalayan region leads to the choice of

two pairs, marked in colours by pairing, in Figure 5.5. The cell pairings that were chosen are such that the difference in their mean elevations is less than $30m$. Unfortunately the Himalayas are not resolved in the run without the subgrid hypsometric parameterisation and so a comparison of the cells with that model can not be made, except that the temperature at the mean altitude is sufficient to melt all accumulation when considered on a grid scale.

Figure 5.5 shows the thickness of ice that has collected in each subgrid bin. Only one of the cells collects any ice at the mean elevation, most likely due to a strong downward flux caused by a larger range in this cell. This figure is illustrative of several key features of the subgrid hypsometric parameterisation.

Firstly it shows that ice develops in a reasonable way on a subgrid scale: it is not a single anomalous bin that is collecting ice but a series of bins. Secondly, the distribution of subgrid thickness is similar to reality, where thickness increases downslope until an area of large melting occurs. Note that the diffusive relaxation used in parameterisation will exaggerate this slightly. Thirdly, cells which have very similar mean heights and climatic conditions are developing quite different ice thicknesses and distributions because of their subgrid terrain. This directly supports work by Marshall and Clarke (2001), showing the importance of subgrid terrain to the mass balance of a glacier.

Considering the wider selection of subgrid cells in Figure 5.6 it is clear that different processes are being modelled. The Alaskan and Andean cells match very closely with the glacier shape as described in the Himalayan cells, albeit a little more smoothly. The cells taken from the ice sheets, however, cannot be thought of as representative of the actual ice sheets. This is because the topographic data that was supplied to the model was surface elevation, which includes the surface of the ice sheets; thus the ice sheets in the model are much higher than they should be. The Antarctic margin cell, with much greater thickness at lower elevations, suggests that either (i) the sheet margins are too steep in the model or (ii) the flow of ice into this cell from neighbouring cells is too large.

## 5.3   Climate Change Scenarios

Figure 5.3 shows the volume timeseries from the HadCM3 dataset runs, the CRU dataset showed the same responses albeit on a smaller scale. Although the dataset does not include the ice sheets there is still significant over-estimation due to the aforementioned Alaska cell. Excluding this

cell, the control run stabilises at around $0.6m$, with the rest of the other runs spread as they are now, but simply closer together.

The aim of a sensitivity study is to examine how the model responds to changes in its dependency fields, in this case precipitation and temperature. Whilst the figure may be polluted by the Alaskan cell the trend is still clear; lowering the climate by one degree has a similar effect to raising it so there is symmetry. The changes, however, are not linear  an increase of $2\,^{\circ}C$ and 4% in the precipitation field (twice the standard change) does not decrease the volume of glaciers as much as the $1x$ change. The model does not seem to be far from a linear decrease in the $2x$ case so more work is required to clarify this.

As temperature increases, the global glacier sensitivity to temperature appears to decrease. It is not clear whether the same can be said for precipitation, if not then precipitation effects may well become more relevant in the future. Sensitivity tests using the HadCM3 projected changes would help to establish whether the model did follow this trend of a dominating dependence on temperature. It is important to establish this as Church et al (2001) based their sea level rise estimates on the basis that precipitation changes were insignificant enough to be ignored; this further sensitivity investigation, however, lies beyond the scope of this study.

The areal coverage and volume plots showed that most regions undergo a loss of mass of mass to some extent. Figure 5.7 shows the reduction in the fractional ice coverage of a grid cell, for the standard simple climate change scenario. The Himalayas seem to be affected the most, with central Europe affected the least. Central Europe, however, is not properly resolved due to the position of the grid on the Earth which explains why it undergoes the least losses.

The $4\,x\,CO_2$ perturbation applied to the HadCM3 climate has some regional variations and anomalies, such as a singular cell in South America that gains volume. Also, the losses of volume appear to be regionally differentiated with greatest loss in the Northern Hemisphere which relates to the greater warming there (see Figure D.1.

Separating the fields it is clear that the additional precipitation has far less impact than additional temperature. This is a commonly found result but that does not make it correct for this ice sheet model as precipitation and temperature changes are highly localised.

The HadCM3 climate projection and the CRU projection differ sufficiently to give substantially different projections of sea level rise; $0.066\,m$ and $0.029\,m$ respectively. Unfortunately this lowers the confidence in the prediction, but based on the earlier tests is not surprising. For

reference, Church et al. (2001) estimated the contribution to sea level rise from glaciers and ice caps would be $0.5\,mm\,a^{-1}$.
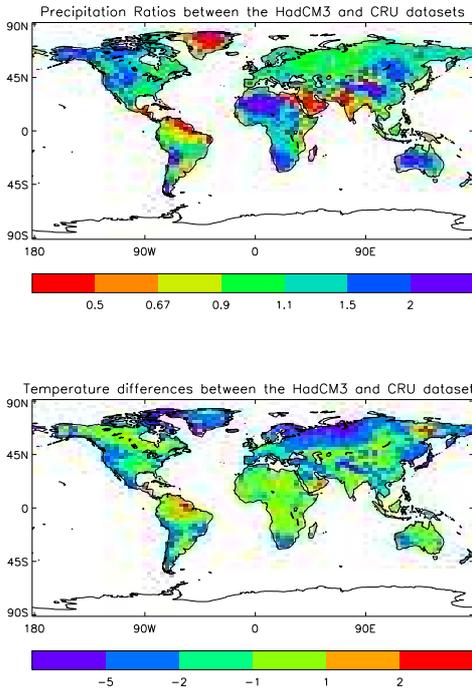
Figure 5.2: The differences in climatology between the HadCM3 and CRU datasets. (a) shows the temperature variations, (b) shows the precipitation variations.
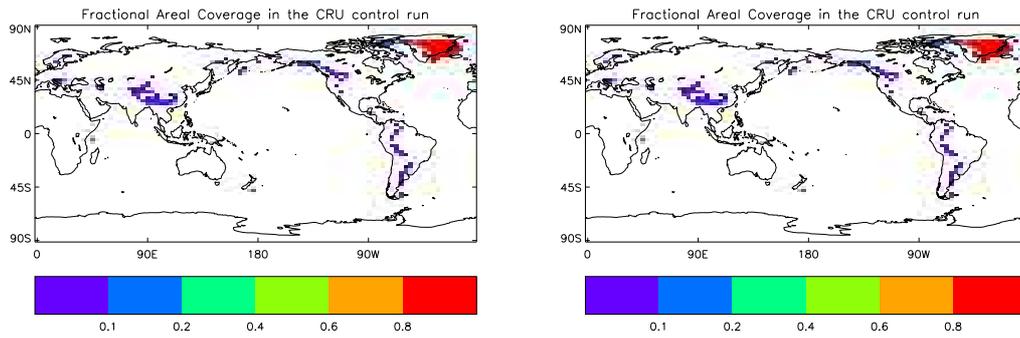
Figure 5.3: Plots of the fraction of areal coverage within each grid-cell.
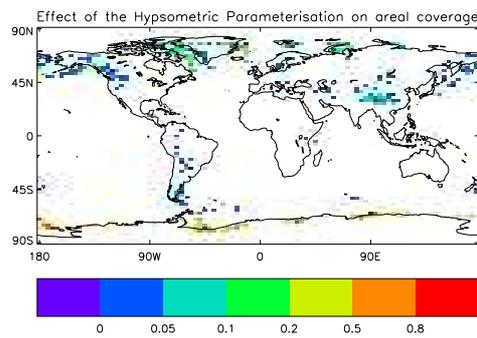


Figure 5.4: Areal ice coverage as a fraction of a grid cell
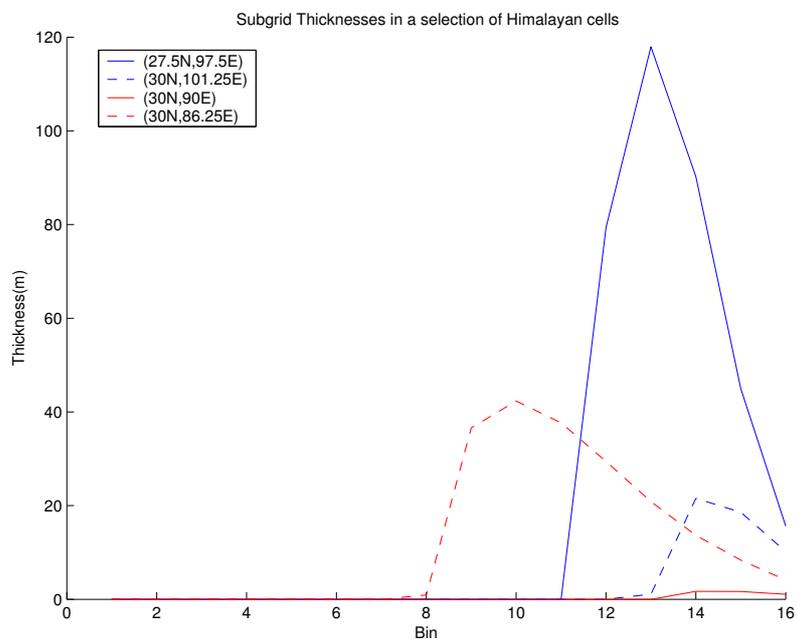
Figure 5.5: From the HadCM3 control run
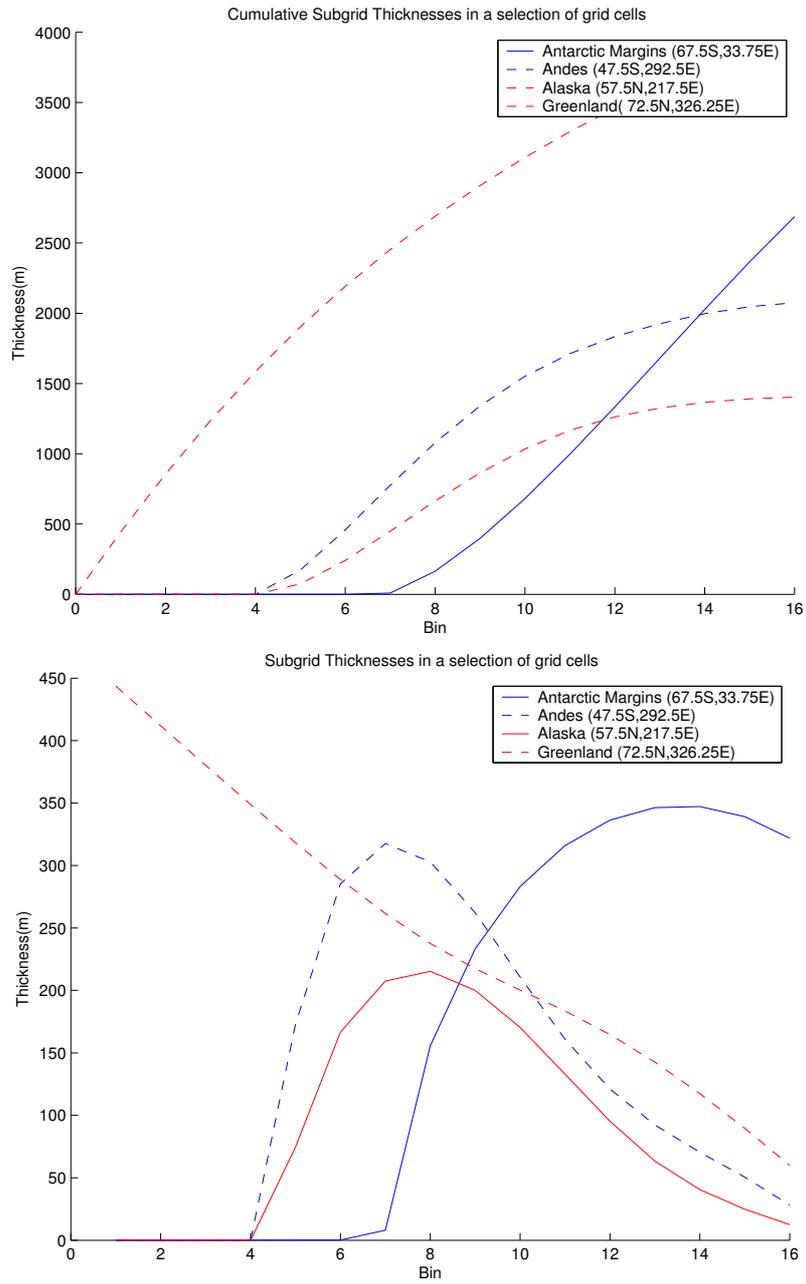
Figure 5.6: Data from the HadCM3 control run

Sensitivity to simple climate change in HadCM3 runs
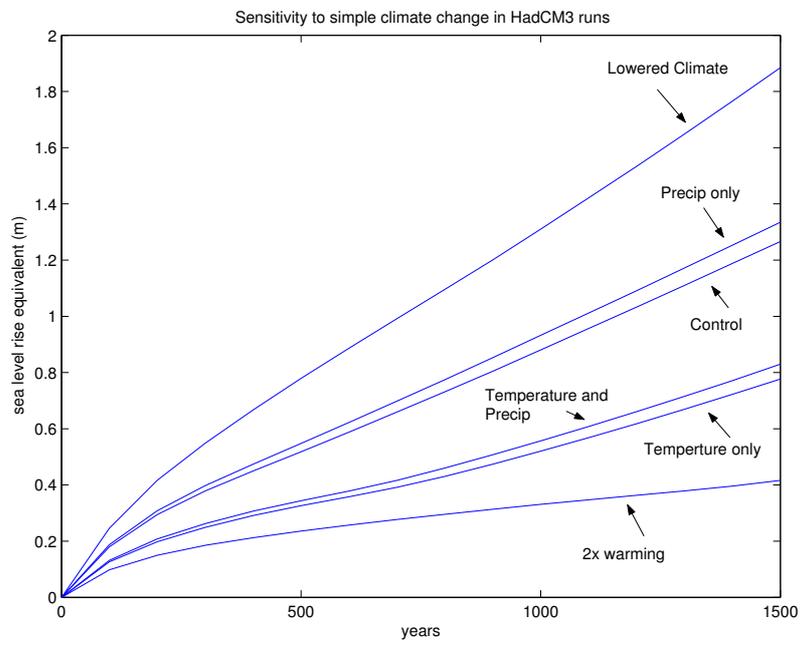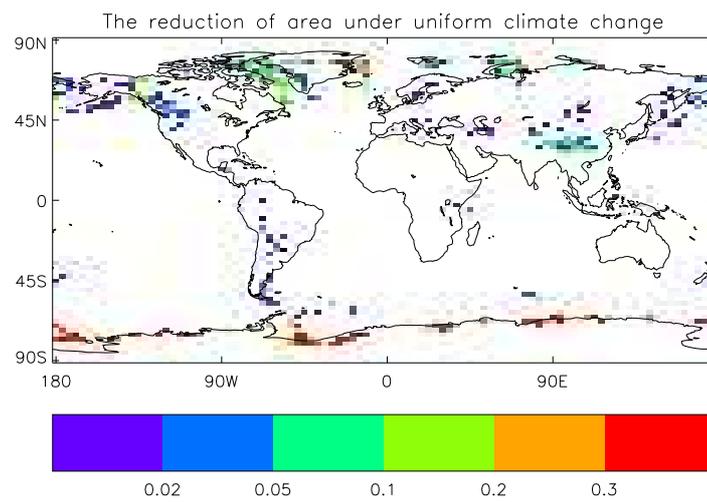
Figure 5.7: CRU datasets, with both a temperature and precipitation increase.

Volume changes,under HadCM3 perturbed climate,in SLR equiv. (mm)
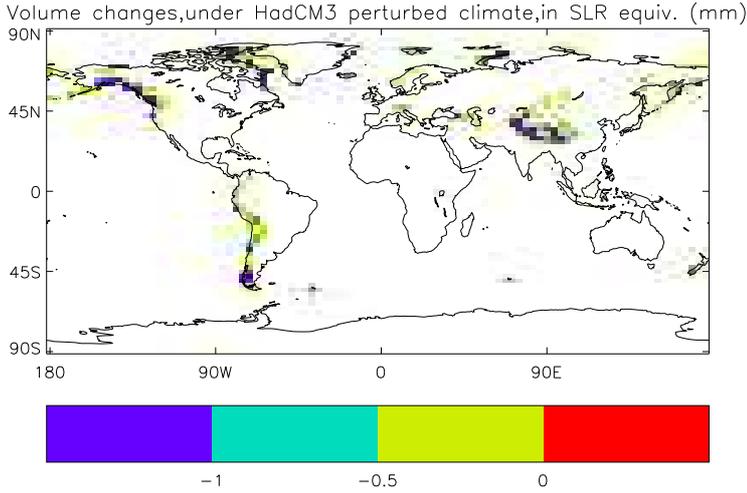


Figure 5.8: From the HadCM3 control run

# Chapter 6

# Conclusions

## 6.1 Summary

The key findings of this study can be summarised in seven points.

1. Inclusion of subgrid topographic detail is essential in order for an ice sheet model to be able to reproduce glaciers on a global scale. The ability to model glaciers accurately with ice sheet models should improve long-term predictions of their contribution to sea level rise.

2. Marshall and Clarkes (2001) subgrid hypsometric parameterisation enables an ice sheet model to reproduce realistic equilibrium states for glaciers. There is much interest in the transient change over coming centuries, as it will be the change that we all feel, but planning for the long-term future requires policy-makers to have an idea of what climate we'll be living in in the future. Whilst this model was not originally designed for modelling equilibrium states, it has been shown to be useful in their consideration.

3. The model is sensitive to the climatology applied. Until HadCM3 or CRU is shown to be the "better" model, there is low confidence in the magnitude of sea level rise predicted in these tests, because of the large range.

4. Under a $4 \times CO_2$ climate change scenario the model predicts that global glacier volume will decrease by $(2.1 \times 10^3 \, km^3)$. This is equivalent to a sea level rise of $66mm$.

5. Glaciers' mass balance is dominated by their sensitivity to temperature changes over precipitation changes. and their relationship

6. If sensitivity to precipitation changes is shown to be significant then this means that the IPCC were wrong to discount it in compiling their predictions of sea level rise.

7. The model shows promise for making practical predictions of global and regional volume and area changes.

## 6.2 Future Work

The HadCM3 dataset and the CRU dataset are sufficiently different to lead to significant differences in the response of the model. It is important, therefore, to determine which of the input data is more accurate in order to improve confidence in the model predictions of sea level change. The regional rather than the global response is more important to many local populations residing in or near glaciated regions.

The climatological data used in these tests was that of a stable climate, the problem with this is firstly that the climate is not stable and secondly that there is greater interest in the transient change than the long term equilibrium response. The use of climatological data that varied over the period of the model run would improve the skill in modelling both the global and regional response to climate change.

There is relatively good data of the recent past ($\sim 500\,yr$) available, in the form of terminal and lateral moraines, and also human records, especially so for communities living near to glaciers. Running the model forward over this period would prove a validation of the skill of the model.

The nature of the differences between the modelled and estimated[1] volumes and areas suggests that the implicit volumearea relationship in Marshall and Clarkes (2001) model is different to the explicit relationship employed by Van de Wal et al. Future work is required to determine which is the correct scaling.

---

[1]Van der Wal et al.

# Appendix A

# References Cited

**Barry**, R.G., (2001). Mountain Weather and Climate. Routledge, London, UK.

**Bahr**, D.B., Meier, M.F., Peckham, S.D., (1997). The physical basis of glacier volume-area saling. Journal of Geophysical Research, 102(B9), 20355-20362.

**Braithwaite**, R., (1984). Calculation of degree-days for glacier-climate research. Zeitschrift für Gletscherkunde und Glazialgeologie, 20, 1-8.

**Braithwaite**, R., (1995). Positive degree-day factors for ablation on the Greenland ice sheet studied by energy-balance modlling. Journal of Glaciology, 41, 153-160.

**Church** J.A., Gregory, J.M., Huybrechts, P., Kuhn, M., Lambeck, K., Nhuan, M.T., Qin, D., Woodworth, P.L., (2001). 'Changes in Sea Level', in Climate Change 2001: The Scientific Basis. Cambridge University Press, Cambridge.

**Dahl-Jenssen**, D., (1989). Steady thermomechanical flow along two-dimensional flow lines in large grounded ice sheets. Journal of Geophysical Research, 94, 10355-10362.

**Erk**, F., (1887). Die vertikale Verteilung und die Maximalzone des Neidershclags am Nordhange der bayrishcen Alpen im Zeitraum November 1883 bis November 1885, Met. Zeit., 4, 44-69.

**Gallee** H., Ypersele van J.P., Fichefet Th, Marsiat I., Tricot Ch., Berger A. (1992). Simulation of the last glacial cycle by a coupled, sectorially averaged climate-ice sheet model. 2. Response to insolation and $CO_2$ variations. Journal of Geophysical Research, 97(D7), 13139-13161.

**Glen**, J.W., (1955). The creep of polycrystaline ice. Proceedings of the Royal Society of London. Series A, 228, 519-538

**Glen**, J.W., (1958). The flow law of ice. A discussion of the assumptions made in glacier theory, their experimental foundations and consequences. IASH 47, 471-183.

**Glover**, R.W, (1998). Influence of spatial resolution and treatment of orography on GCM estimates of the surface mass balance of the Greenland Ice sheet. Journal of Climate, 12(2), 551-563.

**Gordon**, C., Cooper, C., Senior, C. A., Banks, H., Gregory, J. M., Johns, T. C., Mitchell, J. F. B., Wood, R. A., (2000). The Simulation of SST, sea ice extents and ocean heat transports in a version of the Hadley Centre coupled model without flux adjustments. Climate Dynamics, 16, 147-168.

**Hindmarsh**, R.C.A, Payne, A.J. (1996). Time-step limits for stable solutions of the ice-sheet equation. Annals of Glaciology, 23, 74-85.

**Hostetler**, S.W., Clark, P.U., (1997). Climatic controls of western US glaciers at the last glacial maximum. Quaternary Science Reviews, 16, 505-511.

**Jóhannesson**, T., Sigurdsson, O., Laumann, T., Kennett, M., (1995). Degree-day glacier mass-balance modelling with application to glaciers in Iceland, Norway and Greenland. Journal of Glaciology, 41, 345-358.

**Jenssen**, D., (1977). A three-dimensional polar ice-sheet model, J. Glaciol., 18, 373-389.

**Lauer**, W., (1975). Klimatische Grundzüge der Höhenstufung tropischer Gebirge. Tagungsbericht und wissenschatfliche Abhandlungen (p76-90), Innsbruck, F. Steiner.

**Lauscher**, F., (1978). Typen der Höhenabhängigkeit des Niederschlags bei verschiedenen Witterungslagen im Sonnblick Gebiet. Arbieten, Zentralanst, Met. Geodynam., (Vienna), 32(95), 1-6.

**MacAyeal**, D.R. (1989). Large-scale ice flow over a viscous basal sediment: theory and application to Ice Stream B, Antarctica. Journal of Geophysical Research, 94(B4), 4701-4087.

**Mahaffy**, M.W., (1976). A three-dimensional numerical model of ice sheets; test on the Barnes ice cap, Northwest Territories. Journal of Geophysical Research, 81, 1059-1066.

**Marshall**, S.J. (1996). Modelling Laurentide Ice Stream Thermomechanics. Phd Thesis, University of British Columbia, Vancouver, BC, Canada.

**Marshall**, S.J., Clarke, G.K.C. (1997a). A continuum mixture model of ice stream thermomechanics in the Laurentide Ice Sheet, 1. Theory. Journal of Geophysical Research, 102(B9), 20599-20613.

**Marshall**, S.J., Clarke, G.K.C. (1997b). A continuum mixture model of ice stream thermomechanics in the Laurentide Ice Sheet, 2. Application to the Hudson Ice Stream. Journal of Geophysical Research. 102(B9) 20615-20637.

**Marshall**, S.J. (1997c). UBC Ice Sheet Model Documentation.

**Marshall**, S.J., Clarke, G.K.C. (1999). Ice sheet inception: subgrid hypsometric parameterisation of mass balance in an ice sheet model. Climate Dynamics, 15, 533-550.

**Meier**, M.F., Bahr, D.B., (1996). Counting glaciers: use of scaling methods to estimate the number and size distribution of the glaciers of the world. pp. Glaciers, Ice Sheets, and Volcanoes, 89-94. U.S. Army Corps of Engineers, Cold Regions Research and Engineering Laboratory (CRREL).

**New**, M., Hulme, M., Jones, M., (1999). Representing twentieth-century space-time climate variability. Part I: Development of a 1961-90 mean monthly terrestrial climatology. Journal of Climate, 12, 829-856.

**Oerlemans**, J. (1997). A flowline model for Nigardsbreen, Norway: projection of future glacier length based on dynamics calibration with the historic record. Annals of Glaciology, 24, 382-389.

**Patankar**, S.V., (1980). Numerical Heat Transfer and Fluid Flow. Hemisphere Publishing, New York.

**Patterson**, W.S.B., (1994). The physics of glaciers. Pergamon, Oxford, UK.

**Pattyn**, F., (2003). A new three-dimensional higher-order thermomechanical ice sheet model: Basic sensitivity, ice stream development and ice flow across subglacial lakes. Journal of Geophysical Research, 108(B8), 2382-2396.

**Payne**, T., Huybrechts, P. and The EISMINT Intercomparison Group. (2000). Results from the EISMINT model intercomparison: the effects of thermomechanical coupling. Journal of Glaciology, Vol. 46, No. 153.

**Pollard**, D., (1983). A coupled climate-ice sheet model applied to the Quaternary ice ages. Journal of Geophysical Research, 88(C12), 7705-7718.

**Raper**, S.C.B., Brown, O., Braithwaite, R.J., (2000). A geometric glacier model suitable for sea level change calculations. Journal of Glaciology, 46, 367-368.

**Reeh**, N., (1991). Parameterisation of melt rate and surface temperature on the Greenland Ice Sheet. Polarforschung, 59, 113-128.

**Rial**, J.A., (1999). Pacemaking the ice ages by frequency modulation of Earth's orbital eccentricity. Science, 285, 564-568.

**Ruddiman**, W.F., (2001). Earth's Climate. Freeman, New York, USA.

**Saltzman**, B., (2002). Dynamical Paleoclimatology. Academic Press, London, UK.

**Trenberth**, K.E., (1995). Climate System Modelling. Butler and Tanner, London, Uk.

**Van der Wal**, R.S.W, Wild, M., (2001). Modelling the response of glaciers to climate change, applying volume area scaling in combination with a high-resolution GCM. IMAU report R-01-06, Utrecht University, Netherlands.

**Yoshimori**, M., Weaver, A.J., Marshall, S.J., Clarke, G.K.C. (2001). Climate Dynamics 17, 571-588.

# Appendix B

# Flowcharts

These flowcharts illustrate how particular parts of the core dynamics and thermodynamics are solved.
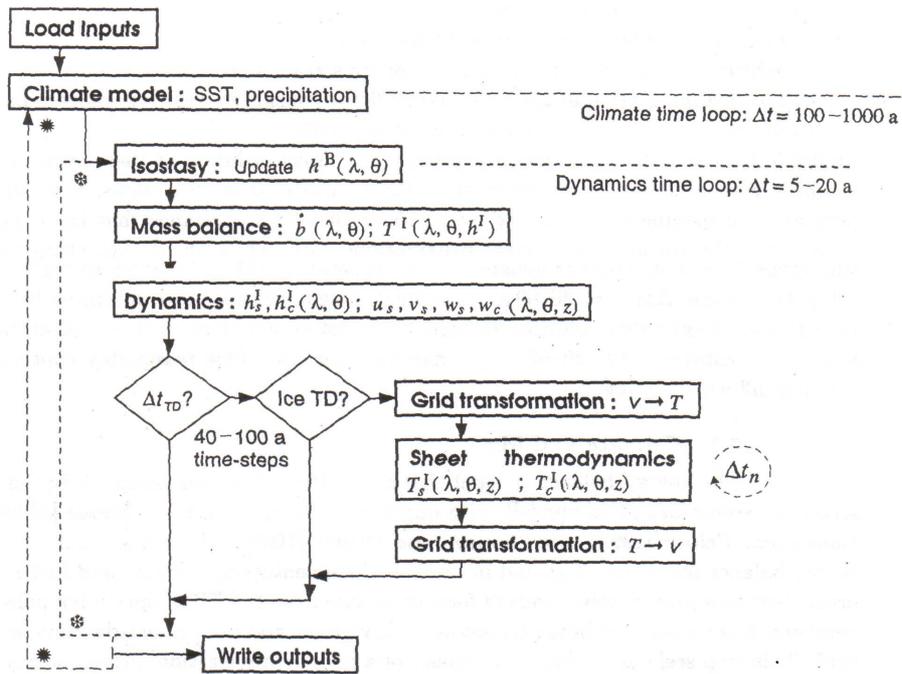


*Flowchart of the core numerical system.*

Figure B.1: from Marshall, (1997c).
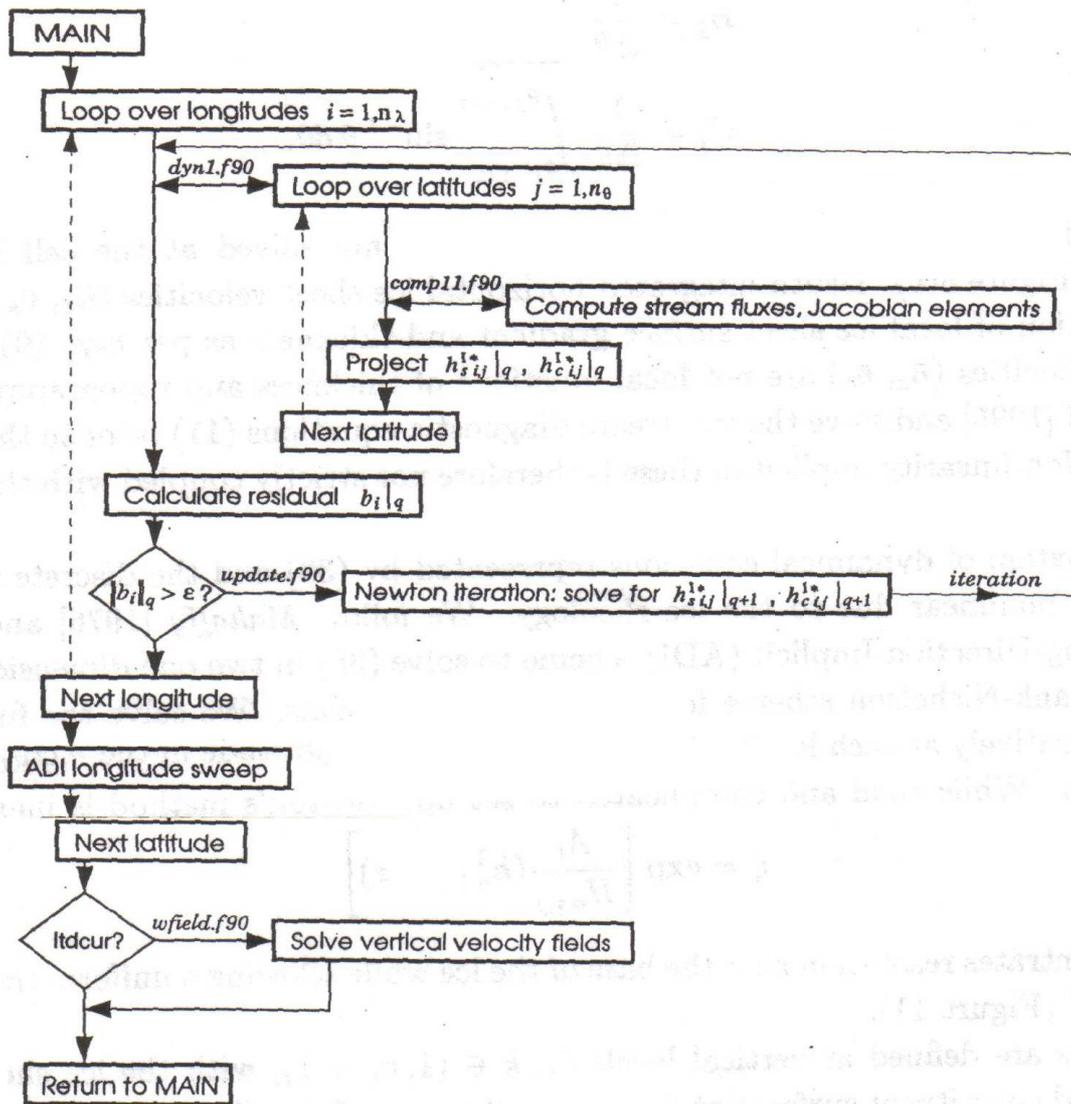
**Figure 10.** *Flowchart of the dynamical system.*

Figure B.2: from Marshall, (1997c).
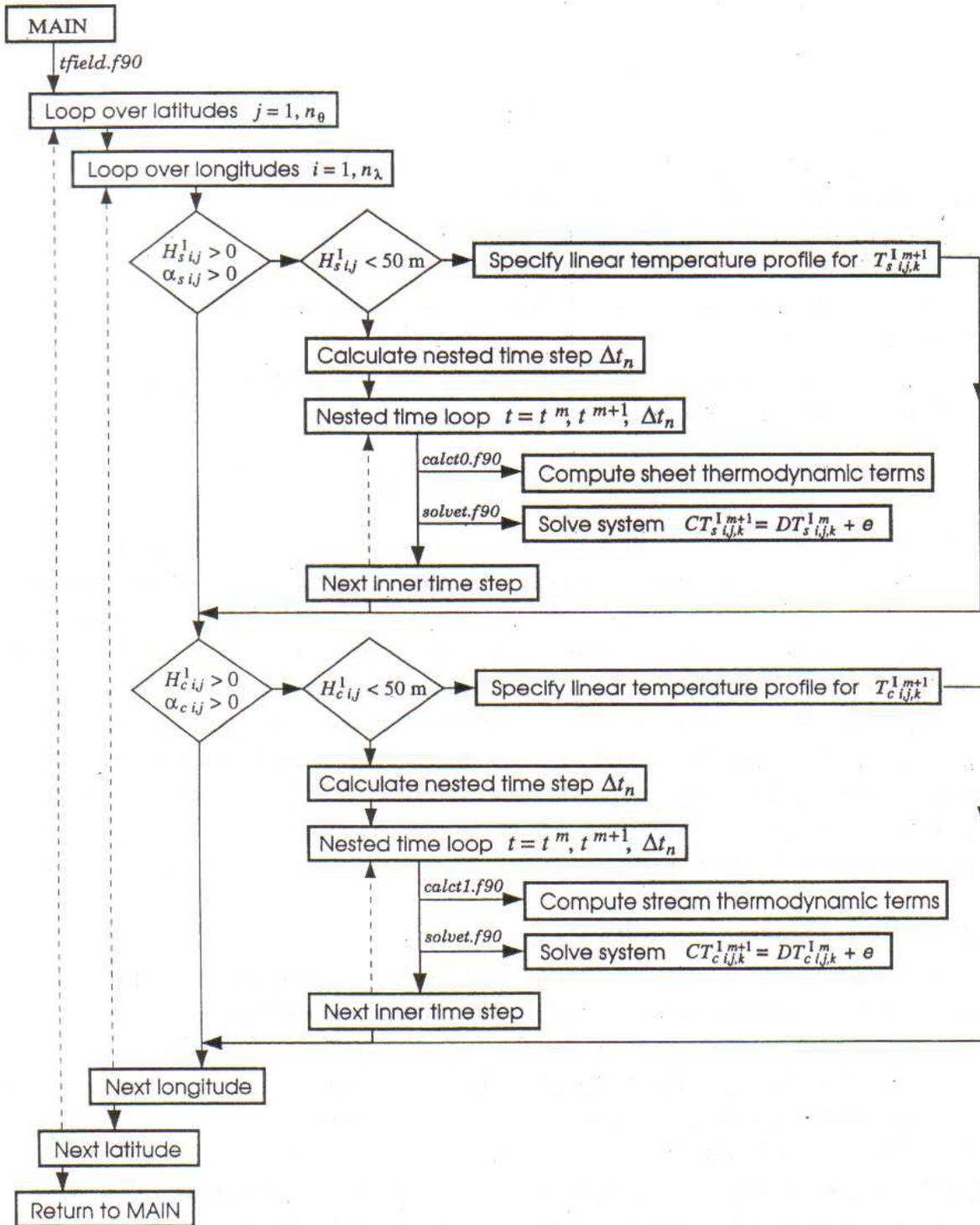
Figure B.3: from Marshall (1997c)

# Appendix C

# Excel charts of Regionalised Data

# Appendix D

# Graphs of HadCM3 Projections of Climate Change

Projected perturbations to the 1860 temperature field by 2100
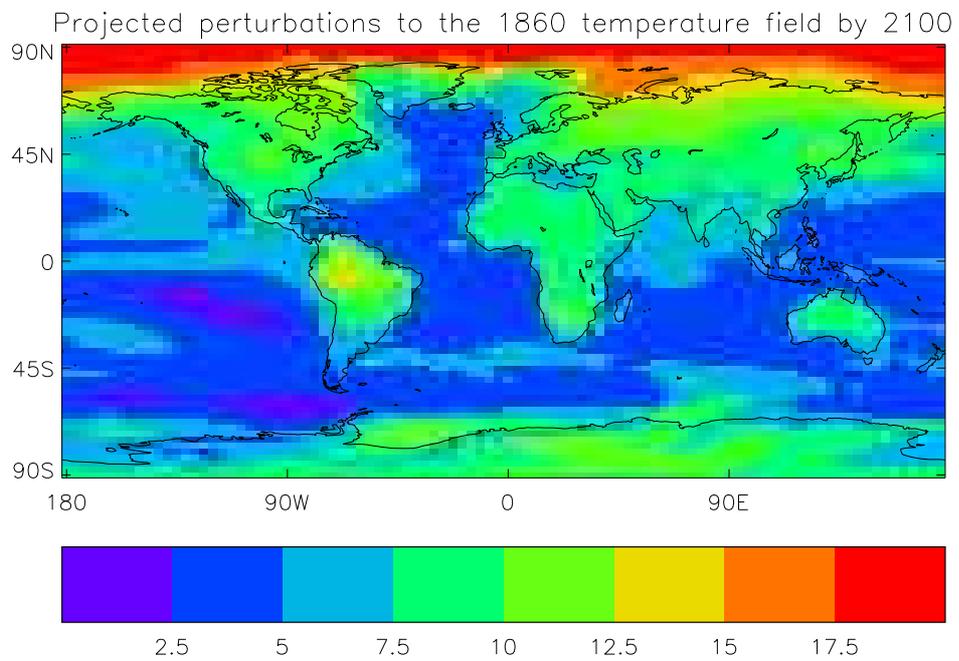
Figure D.1: HadCM3 temperature changes between the 1860-atmospheric-content scenario and the $4xCO^2$ scenario
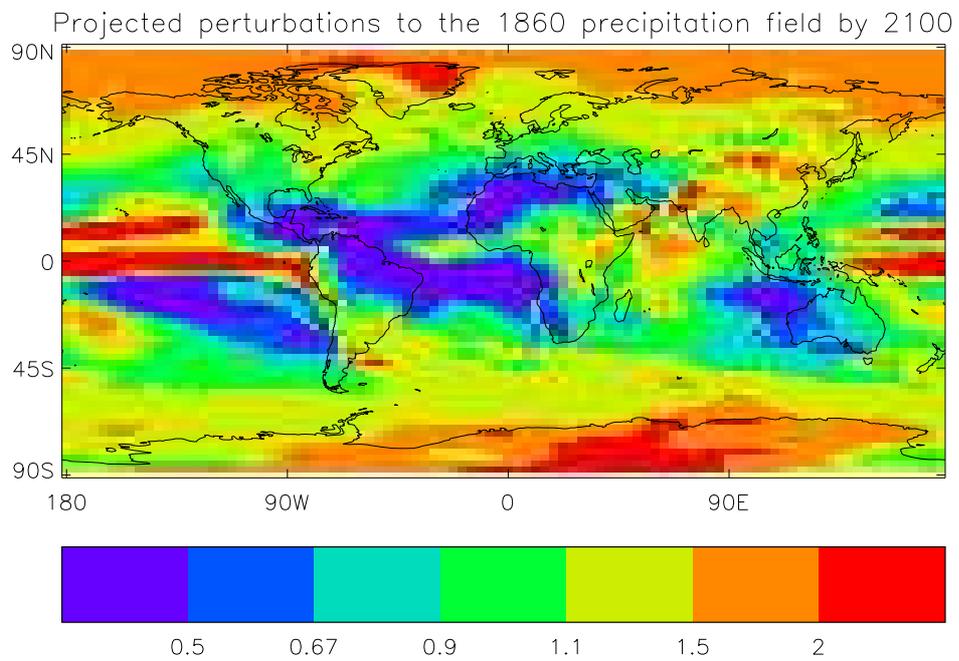
Figure D.2: HadCM3 precipitation changes between the 1860-atmospheric-content scenario and the $4xCO^2$ scenario